Generalized forward–backward initial value representation for the calculation of correlation functions in complex systems

Michael Thoss,[a] Haobin Wang, and William H. Miller
Department of Chemistry and Kenneth S. Pitzer Center for Theoretical Chemistry, University of California, Berkeley, California 94720, and Chemical Sciences Division, Lawrence Berkeley National Laboratory, Berkeley, California 94720

(Received 26 December 2000; accepted 6 February 2001)

The capability of two different, recently proposed semiclassical (SC) forward–backward (FB) initial value representations (IVR) to describe quantum interference and coherence effects is investigated. It is shown that depending on the way the observable under consideration is represented by unitary operators one can obtain rather different results. Although the FB-IVR based on an integral representation as a rule is capable of describing quantum interference, a closer analysis reveals that it depends on the observable under consideration if all interference that can be described semiclassically is actually included in the calculation. To overcome this problem a new, generalized FB-IVR method (GFB-IVR) is proposed, which combines the capability of the SC-IVR to describe quantum interference effects independent of the observable and the better convergence properties of the FB-IVR. The performance of this new approach is studied in some detail. In particular, it is shown that the GFB-IVR can describe both the coherent and incoherent regime in the dynamics of an anharmonic vibration coupled to a harmonic bath. © *2001 American Institute of Physics.*
[DOI: 10.1063/1.1359242]

I. INTRODUCTION

In recent years there has been an increasing interest in semiclassical descriptions of molecular dynamics.[1–59] There are both fundamental and practical reasons why semiclassical methods represent an interesting alternative to quantum mechanical approaches on one hand and purely classical methods on the other hand. Compared to quantum mechanical calculations, semiclassical or classical concepts can often provide a more intuitive, qualitative understanding of the dynamics. It has been shown, for example, that most of the features in simple absorption spectra can be understood by semiclassical dynamics.[16] Being based on classical trajectories, semiclassical approaches are, furthermore, supposed to overcome the exponential scaling with the number of coupled degrees of freedom of straightforward quantum basis-set calculations.[60] Moreover, in contrast to purely classical approaches, semiclassical methods are in principle capable of describing quantum effects such as, for example, interference, zero-point energy conservation, or tunneling processes.[17]

In particular semiclassical (SC) methods based on the initial value representation (IVR) (Ref. 61) (which circumvent the cumbersome root search problem in boundary-value-based semiclassical methods) have been applied successfully to a variety of different problems in molecular dynamics. So far, most of the applications have been limited to rather small systems. The primary problem which prevents a straightforward application to large systems is the oscillatory nature of the integrand involved in the evaluation of the semiclassical propagator. For a high-dimensional system the phase-space integration implicit in the semiclassical propagator is usually done employing Monte Carlo methods. The oscillatory nature of the integrand results in a poor Monte Carlo statistics. This so-called ''sign-problem'' is well known from real-time or fermionic path-integral calculations.[62–65]

Most of the methods proposed so far to overcome this problem[8,11,19,45,48,49] are based on smoothing techniques such as the Filinov[66,67] or stationary-phase Monte Carlo method.[64] The basic idea of this technique is to integrate out the local oscillations analytically using a linearization of the integrand over a small phase-space cell.

A quite different way to circumvent this problem and to facilitate the calculation of correlation functions in complex systems are the various forward–backward methods proposed recently by Miller and co-workers[28,33,36] as well as Makri and co-workers.[68–70] In this approach the smoothing of the integrand is accomplished by combining the forward and backward trajectory for the two propagators in a general correlation function into one forward–backward trajectory with possibly a jump in the momentum of the reaction coordinate. Starting from a full SC-IVR description for the two propagators, which involves a double phase-space integration (see below), the forward–backward (FB) IVR can be obtained by doing one of the integrations within the stationary phase approximation. Therefore, the FB-IVR is more approximate than the full SC-IVR, and the question arises to what extent it can still describe quantum interference effects.

So far there seems to be no unambiguous answer to this question. Gelabert *et al.* have shown recently that the FB-IVR can describe the interference pattern for the double-slit problem qualitatively correctly.[39,71] A similar result has been obtained for quantum coherence effects in the flux-side cor-

[a]Present address: Theoretische Chemie, Technische Universität München, D-85747 Garching, Germany.

relation function for a double well potential[72] as well as for the wave packet dynamics of an anharmonic vibration coupled to a thermal bath.[73] On the other hand, Shao and Makri have shown that a different version of the semiclassical forward–backward propagator cannot describe recurrences in the dynamics of the average position of an anharmonic oscillator.[70]

In the first part of this article we will discuss this problem in some detail and show that it actually depends on the observable under consideration to what extent the FB-IVR can describe quantum interference effects. In the second part we will propose a generalized FB-IVR (GFB-IVR) method which can continuously tune between the full double phase space SC-IVR and the FB-IVR. This flexibility allows one to check if all interference that can be described semiclassically is actually included in the calculation. For the special example of the average position of an anharmonic oscillator we will demonstrate how the recurrences present in the quantum and the full SC-IVR results disappear when the GFB-IVR approaches the FB-IVR. In the last part of the paper we will apply the GFB-IVR to study the quenching of these recurrences when the oscillator is coupled to a bath.

II. DESCRIPTION OF QUANTUM INTERFERENCE IN FB-IVR METHODS

In this section we investigate the capability of two different FB-IVR methods to describe quantum interference effects. To keep the paper self-contained and to facilitate the further discussion we will first give a brief review of semiclassical IVR methods.

The dynamics in complex systems can be described by means of general time-correlation functions[74] such as, for example,

$$C_{AB}(t)=\mathrm{tr}(\hat{A}e^{i\hat{H}t}\hat{B}e^{-i\hat{H}t}). \tag{2.1}$$

Here, $\hat{A}$ and $\hat{B}$ are general operators and $\hat{H}$ denotes the Hamiltonian of the system. (We use units with $\hbar=1$ throughout the paper.) In typical applications, $\hat{A}$ will involve the initial state of the system $\hat{\rho}(0)$ and, therefore, all degrees of freedom, whereas $\hat{B}$ will involve only a few degrees of freedom, e.g., the degrees of freedom that are probed or a reaction coordinate.

To obtain a semiclassical approximation for the correlation function $C_{AB}(t)$ one can insert any semiclassical approximation to the quantum propagator $e^{-i\hat{H}t}$ into Eq. (2.1). In this paper we will use the Herman–Kluk (or coherent state) SC-IVR (Ref. 50) which for a general N-dimensional system reads

$$e^{-i\hat{H}t}=\int\frac{d\mathbf{q}_0 d\mathbf{p}_0}{(2\pi)^N}|\mathbf{q}_t\mathbf{p}_t\rangle C_t(\mathbf{q}_0,\mathbf{p}_0)e^{iS_t(\mathbf{q}_0,\mathbf{p}_0)}\langle\mathbf{q}_0\mathbf{p}_0|. \tag{2.2}$$

Here, $(\mathbf{p}_0,\mathbf{q}_0)$ are initial momenta and coordinates for classical trajectories, $\mathbf{p}_t=\mathbf{p}_t(\mathbf{p}_0,\mathbf{q}_0)$ and $\mathbf{q}_t=\mathbf{q}_t(\mathbf{p}_0,\mathbf{q}_0)$ are the classically time-evolved phase space variables, and S_t is the classical action integral along the trajectory,

$$S_t(\mathbf{q}_0,\mathbf{p}_0)=\int_0^t d\tau(\mathbf{p}_\tau\dot{\mathbf{q}}_\tau-H). \tag{2.3}$$

The pre-exponential factor C_t is given by

$$C_t(\mathbf{p_0},\mathbf{q_0})=\sqrt{\det\left[\frac{1}{2}\left(\boldsymbol{\gamma}^{1/2}\frac{\partial\mathbf{q}_t}{\partial\mathbf{q}_0}\boldsymbol{\gamma}^{-(1/2)}+\boldsymbol{\gamma}^{-(1/2)}\frac{\partial\mathbf{p}_t}{\partial\mathbf{p}_0}\boldsymbol{\gamma}^{1/2}-i\boldsymbol{\gamma}^{1/2}\frac{\partial\mathbf{q}_t}{\partial\mathbf{p}_0}\boldsymbol{\gamma}^{1/2}+i\boldsymbol{\gamma}^{-(1/2)}\frac{\partial\mathbf{p}_t}{\partial\mathbf{q}_0}\boldsymbol{\gamma}^{-(1/2)}\right)\right]}. \tag{2.4}$$

It involves a combination of the elements of the monodromy matrix

$$\mathbf{M}_t=\begin{pmatrix}\frac{\partial\mathbf{p}_t}{\partial\mathbf{p}_0} & \frac{\partial\mathbf{p}_t}{\partial\mathbf{q}_0}\\ \frac{\partial\mathbf{q}_t}{\partial\mathbf{p}_0} & \frac{\partial\mathbf{q}_t}{\partial\mathbf{q}_0}\end{pmatrix}. \tag{2.5}$$

In the above expression $\boldsymbol{\gamma}$ denotes a N-dimensional diagonal matrix, with element γ_j being the width parameter for the coherent state of the jth degree of freedom. The coordinate space representation of an N-dimensional coherent state is the product of N one-dimensional minimum uncertainty wave packets,

$$\langle\mathbf{x}|\mathbf{pq}\rangle=\prod_{j=1}^{N}\left(\frac{\gamma_j}{\pi}\right)^{1/4}e^{-(\gamma_j/2)(x_j-q_j)^2+ip_j(x_j-q_j)}. \tag{2.6}$$

Insertion of the semiclassical propagator (2.2) into Eq. (2.1) gives the full double phase space SC-IVR for the correlation function,

$$\begin{aligned}C_{AB}^{\mathrm{SC}}(t)=\int\frac{d\mathbf{q}_0 d\mathbf{p}_0}{(2\pi)^N}\int\frac{d\mathbf{q}_0' d\mathbf{p}_0'}{(2\pi)^N}C_t(\mathbf{p}_0,\mathbf{q}_0)C_t(\mathbf{p}_0',\mathbf{q}_0')^*\\ \times e^{i[S_t(\mathbf{p}_0,\mathbf{q}_0)-S_t(\mathbf{p}_0',\mathbf{q}_0')]}\langle\mathbf{p}_0\mathbf{q}_0|\hat{A}|\mathbf{p}_0'\mathbf{q}_0'\rangle\\ \times\langle\mathbf{p}_t'\mathbf{q}_t'|\hat{B}|\mathbf{p}_t\mathbf{q}_t\rangle.\end{aligned} \tag{2.7}$$

Here, two trajectories with initial values $(\mathbf{p}_0,\mathbf{q}_0)$ and $(\mathbf{p}_0',\mathbf{q}_0')$ are started at time $t=0$ and then propagated up to time t. C_t and S_t denote the corresponding pre-exponential factor and action, respectively.

For later use we mention that by using Liouville's theorem this expression can be written in a slightly different way, namely,

$$C_{AB}^{\mathrm{SC}}(t)=\int\frac{d\mathbf{q}_0 d\mathbf{p}_0}{(2\pi)^N}\int\frac{d\mathbf{\Delta}_q d\mathbf{\Delta}_p}{(2\pi)^N}C_t(\mathbf{p}_0,\mathbf{q}_0)C_{-t}(\mathbf{p}_t',\mathbf{q}_t')$$
$$\times e^{i[S_t(\mathbf{p}_0,\mathbf{q}_0)+S_{-t}(\mathbf{p}_t',\mathbf{q}_t')]}\langle\mathbf{p}_0\mathbf{q}_0|\hat{A}|\mathbf{p}_0'\mathbf{q}_0'\rangle$$
$$\times\langle\mathbf{p}_t'\mathbf{q}_t'|\hat{B}|\mathbf{p}_t\mathbf{q}_t\rangle. \tag{2.8}$$

In this ''forward–backward'' formulation only a single trajectory with initial values $(\mathbf{p}_0,\mathbf{q}_0)$ is started at $t=0$ and propagated up to time t, where a jump in coordinate and momentum occurs, i.e.,

$$\mathbf{q}_t\rightarrow\mathbf{q}_t'=\mathbf{q}_t+\mathbf{\Delta}_q, \tag{2.9a}$$

$$\mathbf{p}_t\rightarrow\mathbf{p}_t'=\mathbf{p}_t+\mathbf{\Delta}_p, \tag{2.9b}$$

after which the trajectory is propagated back to time $t=0$ with $(\mathbf{p}_0',\mathbf{q}_0')$ being the final phase-space point. In Eq. (2.8), $C_t(\mathbf{p}_0,\mathbf{q}_0)$ and $C_{-t}(\mathbf{p}_t',\mathbf{q}_t')$, as well as $S_t(\mathbf{p}_0,\mathbf{q}_0)$ and $S_{-t}(\mathbf{p}_t',\mathbf{q}_t')$, denote the pre-exponential factors and the actions for the forward and backward trajectory, respectively.

The practical difficulty with the above formulations is that the integrand in the double phase space average is highly oscillatory. In addition, the product of the two pre-exponential factors $C_t(\mathbf{p}_0,\mathbf{q}_0)$ and $C_t(\mathbf{p}_0',\mathbf{q}_0')$ can become large, thereby amplifying the oscillations. To side-step this problem, a linearized approximation to the SC-IVR expression in Eq. (2.7), the LSC-IVR was introduced,[25] whereby all the relevant quantities are expanded to first order in the difference variables $\mathbf{p}_0-\mathbf{p}_0'$ and $\mathbf{q}_0-\mathbf{q}_0'$. The integration over these variables can be carried out analytically, which yields the following much simpler expression for the correlation function

$$C_{AB}^{\mathrm{LSC}}(t)=\int\frac{d\mathbf{q}_0 d\mathbf{p}_0}{(2\pi)^N}A_W(\mathbf{q}_0,\mathbf{p}_0)B_W(\mathbf{q}_t,\mathbf{p}_t). \tag{2.10}$$

Here A_W and B_W are the Wigner function of the operators $\hat{A}$ and $\hat{B}$; i.e., this linearization of the SC-IVR leads to the ''classical Wigner'' model that has arisen before from a variety of approaches.[75–80] Application of this approximation to several interesting models of condensed phase problems was quite successful.[25,27,32] A more thorough analysis, however, showed that the LSC-IVR is able to describe quantum effects only for very short times.[26] For example, it cannot account for the interference pattern in the double-slit problem.[71] It is thus desirable to develop a method that goes beyond this linearized approximation, that can capture the important quantum interference effects, but is still more efficient than evaluating Eq. (2.7).

To this end, Miller and co-workers,[28,33] as well as Makri and co-workers,[68,69] have proposed a ''forward–backward'' (FB) IVR approach for the calculation of time correlation functions. In this approach, the operator product $e^{i\hat{H}t}\hat{B}e^{-i\hat{H}t}$ in Eq. (2.1) is represented by a single Herman–Kluk-type IVR, where the trajectories evolve from time $0\rightarrow t$ (the action of the operator $e^{-i\hat{H}t}$), undergo a momentum (or phase-space) jump at time t (the effect of operator $\hat{B}$), and then evolve backward from $t\rightarrow 0$ (the action of the operator $e^{i\hat{H}t}$). The main advantage of the FB-IVR, besides reducing the dimensionality of the phase space integral, is that there is a partial cancellation of the phase in the integrand and the magnitude of the pre-exponential factor, thus greatly improving the numerical property of the integrand.

To simplify the notation, let us assume that the operator $\hat{B}$ is local in coordinate space, i.e., $\hat{B}=B(\hat{\mathbf{q}})$. [Reference 33 shows how more general operators $B(\hat{\mathbf{q}},\hat{\mathbf{p}})$ as well as the special case when the operator $\hat{B}$ depends on coordinates through a single collective variable $s(\mathbf{q})$, i.e., $B=B(s(\mathbf{q}))$, can be treated.] The existing variants of the FB-IVR method differ primarily in the way the operator $\hat{B}$ is represented by unitary operators. One possibility, which has been used by Miller and co-workers,[28,29,33,36,71,73] is based on the Fourier representation of the operator $\hat{B}$,

$$B(\hat{\mathbf{q}})=\int\frac{d\mathbf{\Delta}_p}{(2\pi)^N}\tilde{B}(\mathbf{\Delta}_p)e^{i\mathbf{\Delta}_p\hat{\mathbf{q}}}. \tag{2.11}$$

The forward–backward IVR for the unitary operator

$$\hat{U}=e^{i\hat{H}t}e^{i\mathbf{\Delta}_p\hat{\mathbf{q}}}e^{-i\hat{H}t} \tag{2.12}$$

can be obtained either by inserting two IVR's for the two propagators and doing the intermediate integration via the stationary phase approximation[81] or by viewing $\hat{U}$ as a single propagator with a time-dependent Hamiltonian.[28,33,36] In both cases the Herman-Kluk FB-IVR for the operator $\hat{U}$ has the same form as Eq. (2.2), and we obtain the following FB-IVR for the correlation function:

$$C_{AB}^{\mathrm{FB}}(t)=\int\frac{d\mathbf{\Delta}_p}{(2\pi)^N}\tilde{B}(\mathbf{\Delta}_p)\int\frac{d\mathbf{q}_0 d\mathbf{p}_0}{(2\pi)^N}C_0(\mathbf{p}_0,\mathbf{q}_0;\mathbf{\Delta}_p)$$
$$\times e^{iS_0(\mathbf{p}_0,\mathbf{q}_0;\mathbf{\Delta}_p)}\langle\mathbf{p}_0\mathbf{q}_0|\hat{A}|\mathbf{p}_0'\mathbf{q}_0'\rangle. \tag{2.13}$$

The FB-IVR trajectory implicit in Eq. (2.13) starts at $t=0$ with initial condition $(\mathbf{p}_0,\mathbf{q}_0)$ and evolves to time t under the molecular Hamiltonian H; at time t the momentum is changed according to

$$\mathbf{p}_t\rightarrow\mathbf{p}_t'=\mathbf{p}_t+\mathbf{\Delta}_p, \tag{2.14}$$

and is then evolved back to time $t=0$ via the molecular Hamiltonian H, (p_0',q_0') being the final phase-space point. The action integral S_0 has contribution from these three time steps,

$$S_0(\mathbf{p}_0,\mathbf{q}_0;\mathbf{\Delta}_p)=\int_0^t d\tau[\mathbf{p}_\tau\cdot\dot{\mathbf{q}}_\tau-H]+\mathbf{\Delta}_p\mathbf{q}_t$$
$$+\int_t^0 d\tau[\mathbf{p}_\tau'\cdot\dot{\mathbf{q}}_\tau'-H], \tag{2.15}$$

and the pre-exponential factor C_0 has the same form as Eq. (2.4),

$$C_0(\mathbf{p}_0,\mathbf{q}_0,\mathbf{\Delta}_p)=\sqrt{\det\left[\frac{1}{2}\left(\boldsymbol{\gamma}^{1/2}\frac{\partial\mathbf{q}_0'}{\partial\mathbf{q}_0}\boldsymbol{\gamma}^{-(1/2)}+\boldsymbol{\gamma}^{-(1/2)}\frac{\partial\mathbf{p}_0'}{\partial\mathbf{p}_0}\boldsymbol{\gamma}^{1/2}-i\hbar\,\boldsymbol{\gamma}^{1/2}\frac{\partial\mathbf{q}_0'}{\partial\mathbf{p}_0}\boldsymbol{\gamma}^{1/2}+\frac{i}{\hbar}\boldsymbol{\gamma}^{-(1/2)}\frac{\partial\mathbf{p}_0'}{\partial\mathbf{q}_0}\boldsymbol{\gamma}^{-(1/2)}\right)\right]}. \tag{2.16}$$

The forward–backward nature of the trajectory provides several advantages over the conventional SC-IVR expression, Eq. (2.8): First, for a complex molecular system the dimension of the phase space average is greatly reduced. For example, in the case that B depends through a collective coordinate on $\mathbf{q}$ [i.e., $\hat{B}=B(s(\hat{\mathbf{q}}))$], the $4N$-dimensional double phase space integration reduces to a $2N$-dimensional single-phase space integration plus a one-dimensional integral over the momentum jump variable. Second, there is a partial cancellation of the phase (those of the action integrals, of the coherent states, and also of the complex pre-exponential factors) which makes the integrand much less oscillatory. Third, there is also a partial cancellation of the magnitude of the pre-exponential factor such that it rarely becomes too large, even for a strongly chaotic system.

A different forward–backward method, which has been proposed by Shao and Marki[70,82] (see also Ref. 33), is based on a derivative representation of the operator $\hat{B}$,

$$\hat{B}=-i\left[\frac{\partial}{\partial\Delta_p}e^{i\Delta_p\hat{B}}\right]_{\Delta_p=0}. \tag{2.17}$$

To simplify the notation we have assumed here that B is a scalar and, therefore, the momentum jump is one-dimensional. Inserting this representation into Eq. (2.1) and using the FB-IVR for the unitary operator $\hat{U}=e^{i\hat{H}t}e^{i\Delta_p\hat{B}}e^{-i\hat{H}t}$, the following forward–backward expression for the correlation function is obtained:

$$C_{AB}^{\mathrm{DFB}}(t)=-i\left[\frac{\partial}{\partial\Delta_p}\int\frac{d\mathbf{q}_0d\mathbf{p}_0}{(2\pi)^N}C_0(\mathbf{p}_0,\mathbf{q}_0;\Delta_p)\times e^{iS_0(\mathbf{p}_0,\mathbf{q}_0;\Delta_p)}\langle\mathbf{p}_0\mathbf{q}_0|\hat{A}|\mathbf{p}_0'\mathbf{q}_0'\rangle\right]_{\Delta_p=0}. \tag{2.18}$$

Similar to Eqs. (2.15) and (2.14), here the action is defined by

$$S_0(\mathbf{p}_0,\mathbf{q}_0;\Delta_p)=\int_0^t d\tau[\mathbf{p}_\tau\cdot\dot{\mathbf{q}}_\tau-H]+\Delta_pB(\mathbf{q}_t)+\int_t^0 d\tau[\mathbf{p}_\tau'\cdot\dot{\mathbf{q}}_\tau'-H], \tag{2.19}$$

and the momentum jump is given by

$$\mathbf{p}_t\rightarrow\mathbf{p}_t'=\mathbf{p}_t+\Delta_p\frac{\partial B}{\partial\mathbf{q}_t}. \tag{2.20}$$

Makri *et al.* have shown that the pre-exponential factor C_0 in Eq. (2.18) can actually be eliminated, thus greatly reducing the numerical effort to calculate the semiclassical correlation function.[70,82] As is outlined in Appendix A, expression (2.18) can be cast into an even simpler form which neither involves the pre-exponential factor nor the action

$$C_{AB}^{\mathrm{DFB}}(t)=\int\frac{d\mathbf{q}_0d\mathbf{p}_0}{(2\pi)^N}B(\mathbf{q}_t)\times\left[1-\frac{1}{4}\sum_j\left(\gamma_j\frac{\partial^2}{\partial q_{0j}^2}+\frac{1}{\gamma_j}\frac{\partial^2}{\partial p_{0j}^2}\right)\right]A_H(\mathbf{q}_0,\mathbf{p}_0). \tag{2.21}$$

Here, A_H denotes the Husimi distribution[83] of the operator $\hat{A}$

$$A_H(\mathbf{p}_0,\mathbf{q}_0)=\langle\mathbf{p}_0\mathbf{q}_0|\hat{A}|\mathbf{p}_0\mathbf{q}_0\rangle. \tag{2.22}$$

Taking into account the relation between the Husimi distribution and the Wigner function,[84]

$$A_W(\mathbf{q}_0,\mathbf{p}_0)=\exp\left[-\frac{1}{4}\sum_j\left(\gamma_j\frac{\partial^2}{\partial q_{0j}^2}+\frac{1}{\gamma_j}\frac{\partial^2}{\partial p_{0j}^2}\right)\right]\times A_H(\mathbf{q}_0,\mathbf{p}_0), \tag{2.23}$$

it is obvious that the terms in brackets in Eq. (2.21) are the first two terms of the series expansion of the operator

$$\exp\left[-\frac{1}{4}\sum_j\left(\gamma_j\frac{\partial^2}{\partial q_{0j}^2}+\frac{1}{\gamma_j}\frac{\partial^2}{\partial p_{0j}^2}\right)\right].$$

The derivative FB-IVR can thus be thought of as an approximate version of the LSC-IVR/classical Wigner model and, therefore, cannot be expected to describe quantum interference beyond the short time limit.[85] This is indeed what Shao and Makri have found for the dynamics of an anharmonic oscillator.[70]

To illustrate this finding, Fig. 1 shows the interference pattern for a simple two-dimensional double-slit problem (for a detailed description of the problem and the parameters,

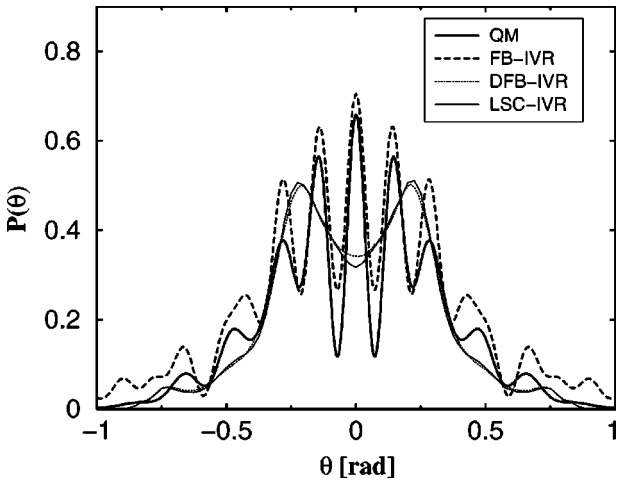

FIG. 1. Angular distribution for a particle passing through a two-slit potential (see Ref. 71 for more details about this example). Shown are quantum mechanical (full line), FB-IVR (dashed line), derivative version of the FB-IVR (dotted line), and LSC-IVR/classical Wigner (thin full line) results.

see Ref. 71). The plot depicts the angular probability distribution after the particle has gone through the slit. The FB-IVR is seen to reproduce the interference pattern qualitatively correctly. The result of the derivative FB-IVR, on the other hand, is nearly indistinguishable from the LSC-IVR/classical Wigner model calculation which cannot describe the interference pattern at all but gives the classical result.

The inability of the derivative FB-IVR to account for the interference can be rationalized in different ways. Considering expression (2.21), which for the angular probability of the double-slit reads

$$P_t(\theta)=\int \frac{d\mathbf{q}_0 d\mathbf{p}_0}{(2\pi)^2}\,\delta(\theta-\theta(\mathbf{q}_t,\mathbf{p}_t)) \times\left[1-\frac{1}{4}\sum_j\left(\gamma_j\frac{\partial^2}{\partial q_{0j}^2}+\frac{1}{\gamma_j}\frac{\partial^2}{\partial p_{0j}^2}\right)\right]A_H(\mathbf{q}_0,\mathbf{p}_0), \tag{2.24}$$

where θ denotes the polar angle [$\theta=\arctan(y/x)$], it is obvious that in this method only a classical average over paths which go through different slits is used, without accounting for the different phase. The drastic difference in the results obtained with the FB-IVR and its derivative form can also be understood from the momentum jump involved in the two different methods. A closer inspection shows that within the FB-IVR the interference pattern is obtained by trajectories that start on the left side of the double-slit, go through one slit, get a momentum kick such that they return through the other slit to the left side. The quantitative analysis reveals that trajectories with a momentum kick of about $40\hbar$ contribute most to the interference pattern. The derivative FB-IVR, on the other hand, only involves infinitesimal momentum jumps, i.e., the trajectories return through the same slit to the left side [cf. Eq. (2.18)] and, therefore, cannot account for the interference.

In the FB-IVR, which is based on an integral representation of the operator $\hat{B}$ [cf. Eq. (2.11)], it depends on the Fourier-transform $\tilde{B}(\mathbf{\Delta}_p)$, and hence on the observable $\hat{B}$, which range of momentum jumps will actually contribute to the dynamics. In the double-slit problem, the observable is the angular probability represented by the delta function operator $\hat{B}=\delta(\theta-\hat{\theta})$. The Fourier transform $\tilde{B}(\Delta_p)=e^{-i\Delta_p\theta}$ is totally delocalized, and therefore all momentum jumps can actually contribute.

The opposite limit pertains for the position operator, $\hat{B}=\hat{q}$ (e.g., to calculate the position autocorrelation function $\langle\hat{q}\hat{q}_t\rangle$ or the average position $\langle\hat{q}_t\rangle$). In this case the Fourier transform is the derivative of a delta function [$\tilde{B}(\Delta_p)=i\delta'(\Delta_p)$], which is highly localized. In fact, in this special case the integral representation (2.11) is equivalent to the derivative representation (2.17) and, therefore, can also not describe quantum interference.

To illustrate this dependence on the observable further, let us consider a simple anharmonic oscillator with the following Hamiltonian (in dimensionless units):

$$H=\frac{p_x^2}{2}+\frac{1}{2}\omega^2x^2+ax^3+bx^4. \tag{2.25}$$

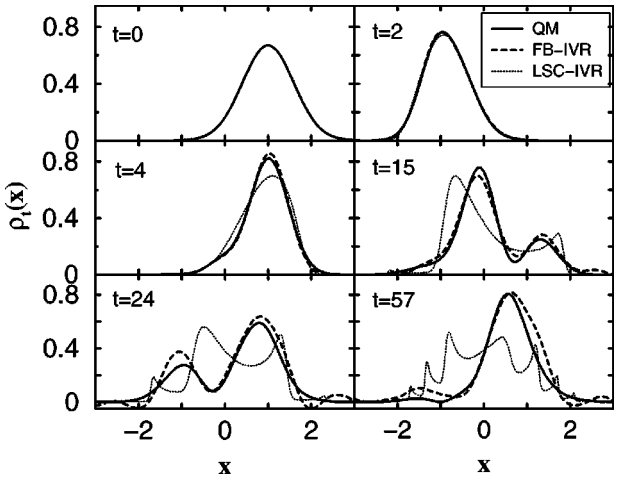

FIG. 2. Snapshots of the wave packet dynamics of an anharmonic oscillator. Shown are quantum mechanical (full line), FB-IVR (dashed line), and LSC-IVR/classical Wigner (thin dotted line) results for the time-dependent density [defined by Eq. (2.27)].

This model has been used by Shao and Makri to demonstrate the performance of the derivative FB-IVR method.[70] The frequency of the oscillator is $\omega=\sqrt{2}$, and the anharmonicity parameters are $a=-0.1, b=0.1$. The initial state is the shifted ground state of the corresponding harmonic oscillator

$$\langle x|\psi_i\rangle=\left(\frac{\gamma}{\pi}\right)^{1/4}e^{-(\gamma/2)(x-1)^2} \tag{2.26}$$

with the width $\gamma=\omega$.

Let us first consider the dynamics of the density (i.e., the time-dependent probability distribution in position)

$$\rho_t(x)=\langle\psi_i|e^{i\hat{H}t}\delta(x-\hat{x})e^{-i\hat{H}t}|\psi_i\rangle. \tag{2.27}$$

In this case operator $\hat{A}$ is the projector onto the initial state ($\hat{A}=|\psi_i\rangle\langle\psi_i|$) and operator $\hat{B}$ projects onto position x. Just as for the angular probability in the double-slit problem, the Fourier transform of $\hat{B}$ is totally delocalized, and we therefore expect a rather good description of quantum interference/coherence effects. This is confirmed by the numerical results in Fig. 2, which shows snapshots of the density. After a short period of essentially classical dynamics, the wave packet splits and dephases due to the anharmonicity of the potential. Later a partial rephasing of the wave packet is observed. This dephasing/splitting and rephasing of a wave packet is based on quantum interference and cannot be described by a more classical method such as the LSC-IVR (shown by the thin lines) or the derivative FB-IVR (which is not shown, but is found to be nearly indistinguishable from the LSC-IVR result). The FB-IVR, on the other hand, is seen to be in rather good agreement with the quantum result.

A more compact description of the wave packet recurrences can be obtained by the normalized autocorrelation function of the density,

$$J(t)=\frac{\int dx\,\rho_t(x)\rho_0(x)}{\int dx\,\rho_0^2(x)}. \tag{2.28}$$

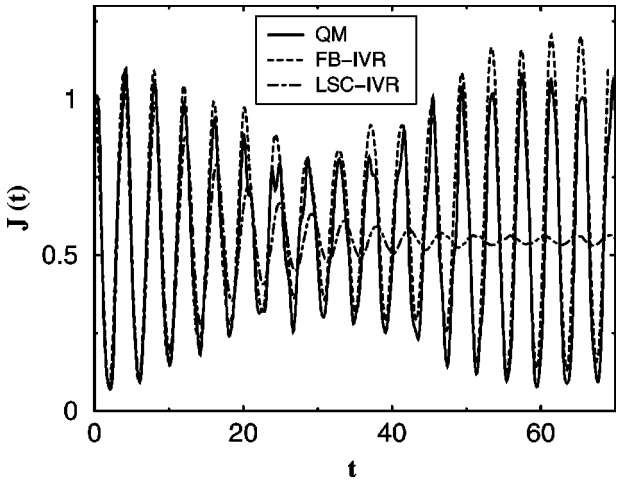

FIG. 3. Density autocorrelation function of an anharmonic oscillator [as defined by Eq. (2.28)]. Shown are quantum mechanical (full line), FB-IVR (dashed line), and LSC-IVR/classical Wigner (dashed–dotted line) results.

This quantity is depicted in Fig. 3. It shows a pronounced recurrence at $t \approx 60$. The FB-IVR is seen to be in very good agreement with the quantum result, whereas the LSC-IVR totally fails to describe the recurrence.

Let us next consider the average position

$$\langle x \rangle_t = \langle \psi_i | e^{i\hat{H}t} \hat{x} e^{-i\hat{H}t} | \psi_i \rangle, \tag{2.29}$$

which corresponds to the first moment of the density $\rho_t(x)$. Figure 4 displays the numerical results of the quantum mechanical, SC-IVR, and FB-IVR calculations, respectively. For a harmonic oscillator, this observable would oscillate between 1 and -1 indefinitely. As was shown above, the anharmonicity leads to a dephasing/splitting of the wave packet, which becomes manifest in a smaller amplitude of the oscillation at $t \approx 25$. Later the wave packet rephases to some extent which leads to a recurrence in $\langle x \rangle_t$ at $t \approx 60$. Because for $\hat{B} = \hat{x}$ the FB-IVR is equivalent to the derivative FB-IVR (which in turn is close to the LSC-IVR), it cannot describe this rephasing process correctly, as can be seen in Fig. 4. The full SC-IVR, on the other hand, is in excellent agreement with the quantum results, thus demonstrating that the failure of the FB-IVR is caused by the additional stationary phase approximation used in the derivation of the FB-IVR.

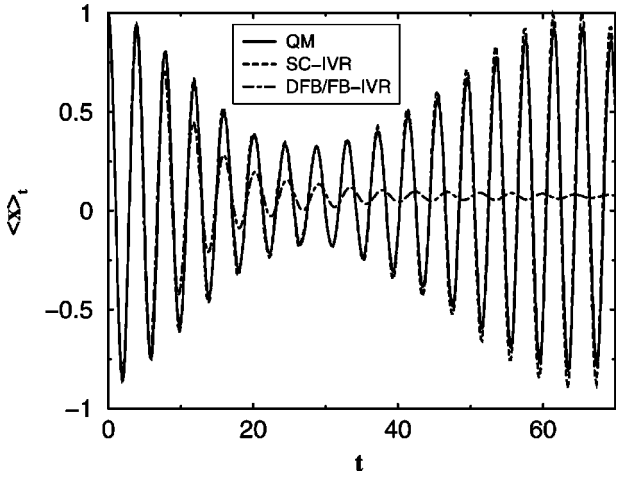

FIG. 4. Dynamics of the average position of an anharmonic oscillator [cf. Eq. (2.29)]. Shown are quantum mechanical (full line), full SC-IVR (dashed line), and FB-IVR (dashed–dotted line) results.

As the dimension of the system increases, it becomes more and more difficult to converge the double phase space integral of the full SC-IVR expression (2.7). Therefore, one would like to have a method which combines the better convergence properties of the FB-IVR and the capability of the SC-IVR to describe quantum interference effects independent of the observable under consideration. Such a *generalized* FB-IVR approach is proposed in the next section.

III. GENERALIZED FB-IVR METHOD

In this section we present a generalized FB-IVR (GFB-IVR) method which (as a function of a certain parameter) can tune continuously between the two limiting cases of the full double phase space SC-IVR and the FB-IVR. The derivation of this method is based on a modified Filinov transformation[66,67] which has been used before to smooth out oscillatory integrands occurring in SC-IVR calculations.[19]

To briefly review the basic idea of the Filinov transformation let us consider the integral

$$I = \int d\mathbf{z}\, g(\mathbf{z}) e^{if(\mathbf{z})}, \tag{3.1}$$

where the functions f,g are in general complex. Due to the phase factor $e^{if(z)}$ the integrand is oscillatory and therefore difficult to integrate with Monte Carlo methods. The modified Filinov method approximates the integral (3.1) by the expression

$$I \approx I(\mathbf{c}) = \int d\mathbf{z} g(\mathbf{z}) e^{if(\mathbf{z})} \sqrt{\det\left(1 + i\mathbf{c}\frac{\partial^2 f}{\partial \mathbf{z}\partial \mathbf{z}}\right)} \times \exp\left(-\frac{1}{2}\frac{\partial f}{\partial \mathbf{z}}\mathbf{c}\frac{\partial f}{\partial \mathbf{z}}\right), \tag{3.2}$$

where $\mathbf{c}$ is the matrix containing the Filinov parameters.[67] In general the choice of this matrix is rather arbitrary. To simplify the discussion let us assume for the moment that $\mathbf{c} = c\mathbf{1}$. Then for $c = 0$ one regains the original integral (3.1). In the opposite limit, i.e., $c \to \infty$, the integral in Eq. (3.2) approaches the stationary phase approximation to I,

$$I_{\mathrm{SPA}} = \sum_j g(\mathbf{z}_j) e^{if(\mathbf{z}_j)} \sqrt{\det\left(2\pi i \Big/ \frac{\partial^2 f}{\partial \mathbf{z}\partial \mathbf{z}}\right)}, \tag{3.3}$$

where the sum goes over all points of stationary phase. For finite values of c the modified Filinov transformation results in a smoothing of the integrand which in turn leads to better Monte Carlo statistics.

Applying the modified Filinov method to the full SC-IVR expression (2.7) gives the following GFB-IVR for the correlation function $C_{AB}(t)$ (the details of the derivation are outlined in Appendix B):

$$C_{AB}^{\mathrm{GFB}}(t)=\int\frac{d\mathbf{q}_0 d\mathbf{p}_0}{(2\pi)^N}\int\frac{d\mathbf{\Delta}_q d\mathbf{\Delta}_p}{(2\pi)^N}\langle\mathbf{p}_0\mathbf{q}_0|\hat{A}|\mathbf{p}_0'\mathbf{q}_0'\rangle$$
$$\times e^{i[S_t(\mathbf{p}_0,\mathbf{q}_0)+S_{-t}(\mathbf{p}_t',\mathbf{q}_t')]}$$
$$\times\overline{C}_0(\mathbf{p}_0,\mathbf{q}_0;\mathbf{\Delta}_p,\mathbf{\Delta}_q)e^{-(1/2)\mathbf{\Delta}_q\mathbf{c}_q\mathbf{\Delta}_q}\langle\mathbf{p}_t'\mathbf{q}_t'|\hat{\tilde{B}}|\mathbf{p}_t\mathbf{q}_t\rangle. \tag{3.4}$$

The trajectories implicit in Eq. (3.4) are the same as in the full SC-IVR (2.8), i.e., the trajectories are started at $t=0$ with initial values $(\mathbf{p}_0,\mathbf{q}_0)$ and propagated up to time t, where a jump in coordinate and momentum occurs [cf. Eq. (2.9)], after which they are propagated back to time $t=0$ (with final values $\mathbf{p}_0',\mathbf{q}_0'$). $S_t(\mathbf{p}_0,\mathbf{q}_0)$ and $S_{-t}(\mathbf{p}_t',\mathbf{q}_t')$ denote the action for the forward and backward part of the trajectory, respectively. To simplify the notation and discussion we have again assumed (as in Sec. II) that the operator $\hat{B}$ is local in coordinate space, i.e., $\hat{B}=B(\hat{\mathbf{q}})$. The result for a general operator $\hat{B}=B(\hat{\mathbf{q}},\hat{\mathbf{p}})$ is given in Appendix B. The operator $\hat{\tilde{B}}$ in Eq. (3.4) is related to $\hat{B}$ via its Fourier transform $\tilde{B}(\mathbf{\Delta}_p)$ through the following convolutive expression:

$$\hat{\tilde{B}}=\int\frac{d\mathbf{p}'}{(2\pi)^N}\tilde{B}(\mathbf{p}')e^{i\mathbf{p}'\hat{\mathbf{q}}}e^{-(1/2)(\mathbf{\Delta}_p-\mathbf{p}')\mathbf{c}_p(\mathbf{\Delta}_p-\mathbf{p}')}. \tag{3.5}$$

The difference from the original operator $\hat{B}$ [cf. Eq. (2.11)], i.e., the convolution with a Gaussian, is due to the Filinov transformation applied to the matrix element $\langle\mathbf{p}_t'\mathbf{q}_t'|\hat{B}|\mathbf{p}_t\mathbf{q}_t\rangle$. The pre-exponential factor $\overline{C}_0$ is given by

$$\overline{C}_0(\mathbf{p}_0,\mathbf{q}_0;\mathbf{\Delta}_p,\mathbf{\Delta}_q)$$
$$=2^{-N}\left\{\frac{\det[(1+\overline{\mathbf{c}}_q)(1+\overline{\mathbf{c}}_p)-1]}{\det(\gamma)}\det(\mathbf{D})\right\}^{1/2}, \tag{3.6}$$

where the matrix $\mathbf{D}$ involves the monodromy matrix elements for the forward and backward part of the trajectory and is defined in Eq. (B20) in Appendix B. The diagonal matrices $\overline{\mathbf{c}}_q,\overline{\mathbf{c}}_p$ contain the γ-scaled Filinov parameters

$$\overline{\mathbf{c}}_q=2\gamma^{-1}\mathbf{c}_q,\quad \overline{\mathbf{c}}_p=2\gamma\mathbf{c}_p. \tag{3.7}$$

It is instructive to discuss two limiting cases. In the limit $\mathbf{c}_q=\mathbf{c}_p=0$, the pre-exponential factor $\overline{C}_0$ can be written as a product of the two pre-exponential factors for the forward and backward trajectory, i.e.,

$$\overline{C}_0(\mathbf{p}_0,\mathbf{q}_0;\mathbf{\Delta}_p,\mathbf{\Delta}_q)=C_t(\mathbf{p}_0,\mathbf{q}_0)C_{-t}(\mathbf{p}_t',\mathbf{q}_t'),$$
$$\text{for}\quad \mathbf{c}_q=\mathbf{c}_p=0, \tag{3.8}$$

and, furthermore, the identity $\hat{\tilde{B}}=\hat{B}$ holds. Therefore, the GFB-IVR expression reverts to the full double phase space SC-IVR [in the form (2.8)] in this limit.

In the opposite limit, i.e., $\mathbf{c}_q,\mathbf{c}_p\to\infty$, one has

$$[\det(\overline{\mathbf{c}}_q)\det(\overline{\mathbf{c}}_p)]^{-1/2}\overline{C}_0(\mathbf{p}_0,\mathbf{q}_0;\mathbf{\Delta}_q,\mathbf{\Delta}_p)$$
$$\to C_0(\mathbf{p}_0,\mathbf{q}_0,\mathbf{\Delta}_p,\mathbf{\Delta}_q), \tag{3.9}$$

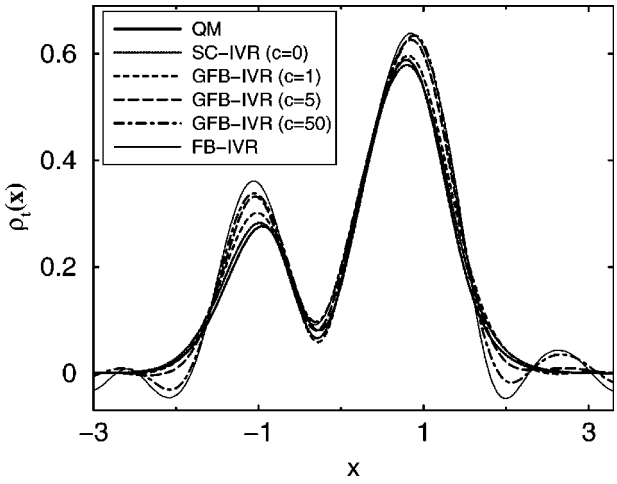

FIG. 5. Density $\rho_t(x)$ for an anharmonic oscillator at time $t=24$. Shown are quantum mechanical (full line), SC-IVR (dotted line), and FB-IVR (thin full line) results as well as GFB-IVR results for different values of the Filinov parameter: $\overline{c}=1$ (short-dashed line), $\overline{c}=5$ (long-dashed line), $\overline{c}=50$ (dashed–dotted line).

where C_0 denotes the FB-IVR pre-exponential factor for the combined forward–backward trajectory [cf. Eq. (2.16)]. Moreover, it is easy to show that

$$[\det(\overline{\mathbf{c}}_q)\det(\overline{\mathbf{c}}_p)]^{1/2}e^{-(1/2)\mathbf{\Delta}_q\mathbf{c}_q\mathbf{\Delta}_q}\langle\mathbf{p}_t'\mathbf{q}_t'|\hat{\tilde{B}}|\mathbf{p}_t\mathbf{q}_t\rangle$$
$$\to\delta(\mathbf{\Delta}_q)\tilde{B}(\mathbf{\Delta}_p)e^{i\mathbf{\Delta}_p\mathbf{q}_t}, \tag{3.10}$$

and, therefore, the GFB-IVR becomes the FB-IVR in the limit $\mathbf{c}_q,\mathbf{c}_p\to\infty$. This is to be expected, since this limit corresponds within the modified Filinov method to the stationary phase approximation.

For finite $\mathbf{c}_q,\mathbf{c}_p$ the GFB-IVR will give a result somewhere in between the full SC-IVR and the FB-IVR. In general, the larger the Filinov parameters $\mathbf{c}_q,\mathbf{c}_p$ are chosen, the smaller is the momentum and coordinate jump and, therefore (as in the case of the FB-IVR), the better are the convergence properties of the Monte Carlo integration.[86] On the other hand, to include all quantum interference effects that can be described by the full SC-IVR one would like to chose a rather small Filinov parameter.

To study the dependence on the parameters $\mathbf{c}_q,\mathbf{c}_p$ let us again consider the anharmonic oscillator with Hamiltonian (2.25). In Sec. II we had already seen that for the time-dependent density $\rho_t(x)$ there is little difference between the full SC-IVR and the FB-IVR result (and both are in rather good agreement with the quantum mechanical result). For the average position, on the other hand, the FB-IVR reduces to the derivative FB-IVR and, hence, cannot describe the recurrences present in the full SC-IVR result (and in the quantum mechanical calculation).

Let us first focus on the density. Figure 5 compares the quantum mechanical result for the density at time $t=24$ with results obtained using the full SC-IVR, the GFB-IVR and the FB-IVR. In all GFB-IVR calculations we have used the same γ-scaled Filinov parameter for coordinate and momentum, i.e., $\overline{c}_q=\overline{c}_p=\overline{c}$. Overall the agreement with the quantum results is seen to be rather good for all semiclassical calcula-

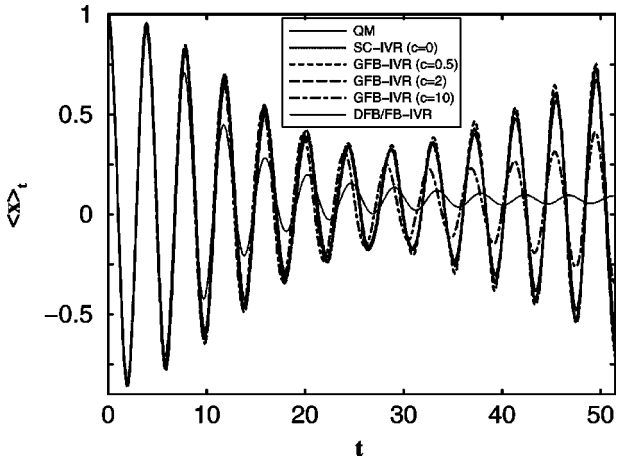

FIG. 6. Dynamics of the average position of an anharmonic oscillator. Shown are quantum mechanical (full line), SC-IVR (dotted line), and FB-IVR (thin full line) results as well as GFB-IVR results for different values of the Filinov parameter: $\bar{c}=0.5$ (short-dashed line), $\bar{c}=2$ (long-dashed line), $\bar{c}=10$ (dashed–dotted line).

tions and there is only a weak dependence on the Filinov parameter $\bar{c}$. The SC-IVR (which corresponds to a GFB-IVR calculation with $\bar{c}=0$) as well as the GFB-IVR calculations with $\bar{c}\leqslant 2$ reproduce the quantum result almost quantitatively. Increasing the Filinov parameter $\bar{c}$ further, the agreement with the quantum result deteriorates to some extent. In particular, for $\bar{c}>2$ part of the density becomes slightly negative.[87] The results in Fig. 5 also illustrate how the GFB-IVR (as a function of $\bar{c}$) can tune continuously between the full SC-IVR and the FB-IVR.

In contrast to this result for the density, there is a rather strong dependence on the parameters $\mathbf{c}_q, \mathbf{c}_p$ for the average coordinate $\langle x\rangle_t$ depicted in Fig. 6. For values $0\leqslant\bar{c}\leqslant 2$ the GFB-IVR agrees rather well with the quantum result and reproduces the recurrence at $t\approx 50$ perfectly. This demonstrates that there is a range of $\bar{c}$-values where all interference effects that can be described semiclassically are included and where the results are rather insensitive to the particular value of $\bar{c}$. Increasing the Filinov parameter further ($\bar{c}>2$), the GFB-IVR results at longer times ($t>20$) deteriorate drastically. For $\bar{c}\to\infty$ it approaches the FB-IVR result which cannot describe the recurrence at all.

This example demonstrates that the GFB-IVR with a proper choice of the Filinov parameter c can describe quantum interference effects independent of the observable. A practical strategy is to do some test calculations for different values of c and then choose c as small as the Monte Carlo statistics allows.

IV. GFB-IVR FOR SYSTEM–BATH PROBLEMS

When treating the dynamics of large molecules or processes in a condensed phase, it is often meaningful to separate the problem into a low-dimensional system (in the simplest case a single reaction coordinate) which is probed and/or responsible for the quantum effects and, therefore, needs to be treated at a higher level of theory, and a bath which provides the dissipative environment and can be treated at a lower level. In this section we will show how the GFB-IVR method proposed in the previous section can be adapted to this situation.

Consider a general Hamiltonian for a system–bath problem,

$$H=H_S+H_B+H_{\mathrm{SB}}$$
$$=\frac{p_x^2}{2}+V_S(x)+\sum_j\left[\frac{P_j^2}{2}+V_B(Q_j)\right]+H_{\mathrm{SB}}, \tag{4.1}$$

where x denotes the system coordinate and p_x the corresponding momentum (to simplify the notation we assume a one-dimensional system); Q_j and P_j are likewise the coordinate and momentum of the jth bath mode. V_S and V_B denote the potential energy for system and bath, respectively, and H_{SB} describes the coupling between them.

Depending on the physical problem under consideration there may be different ways for the separation into system and bath. A rather natural way is to define the system as those degrees of freedom that are probed in the process under consideration. In terms of the correlation function $C_{AB}(t)$, this means that the system is defined by the degrees of freedom on which the operator $\hat{B}$ depends [i.e., $\hat{B}=B(\hat{x})$]. A typical example is the autocorrelation function of a reaction coordinate,

$$C_{xx}(t)=\mathrm{tr}(\hat{\rho}(0)\hat{x}e^{i\hat{H}t}\hat{x}e^{-i\hat{H}t}), \tag{4.2}$$

which (within the linear approximation for the dipole moment) is related to infrared absorption spectrum, or, even simpler, the average value of the reaction coordinate,

$$\langle x\rangle_t=\mathrm{tr}(\hat{\rho}(0)e^{i\hat{H}t}\hat{x}e^{-i\hat{H}t}), \tag{4.3}$$

which was considered above.

The GFB-IVR method can rather naturally be adapted to these types of problems. The GFB-IVR expression for the combined system–bath problem involves, in general, $2N=2N_S+2N_B$ Filinov parameters $\mathbf{c}_{p_x}, \mathbf{c}_x, \mathbf{c}_{pB}, \mathbf{c}_{qB}$. If all these parameters are rather small (or even zero as in the case of the full double phase space SC-IVR) it will be very difficult to converge the Monte Carlo integral in Eq. (3.4). A natural strategy to improve the Monte Carlo statistics is to keep the Filinov parameters for the system degrees of freedom (and possibly for those bath degrees of freedom that are important for quantum effects) as small as the description of quantum interference effects requires, but use a rather large value for the Filinov parameters of the bath (or those bath degrees of freedom that are supposed to be rather classical). The best convergence properties will, of course, be obtained in the limit $\mathbf{c}_{pB}, \mathbf{c}_{qB}\to\infty$, which corresponds to a stationary phase limit for the bath degrees of freedom. In this case the momentum and coordinate jumps disappear for the bath degrees of freedom, i.e., the bath trajectories become continuous. In this limit we obtain the following system–bath GFB-IVR expression for the correlation function:

$$C_{AB}^{\mathrm{GFB}}(t)=\int \frac{d\mathbf{Q}_0 d\mathbf{P}_0}{(2\pi)^{N_B}} \frac{d\mathbf{x}_0 d\mathbf{p}_{\mathbf{x}0}}{(2\pi)^{N_S}} \int \frac{d\mathbf{\Delta}_x d\mathbf{\Delta}_{p_x}}{(2\pi)^{N_S}} \times \langle \mathbf{P}_0\mathbf{Q}_0|\langle \mathbf{p}_{x0}\mathbf{x}_0|\hat{A}|\mathbf{p}'_{x0}\mathbf{x}'_0\rangle|\mathbf{P}'_0\mathbf{Q}'_0\rangle \times e^{i[S_t(\mathbf{p}_0,\mathbf{q}_0)+S_{-t}(\mathbf{p}'_t,\mathbf{q}'_t)]} \times \overline{C}_0(\mathbf{p}_{x0},\mathbf{x}_0,\mathbf{P}_0,\mathbf{Q}_0;\mathbf{\Delta}_x,\mathbf{\Delta}_{p_x}) \times e^{-(1/2)\mathbf{\Delta}_x\mathbf{c}_x\mathbf{\Delta}_x}\langle \mathbf{p}'_{xt}\mathbf{x}'_t|\hat{\bar{B}}|\mathbf{p}_{xt}\mathbf{x}_t\rangle, \quad (4.4)$$

where the pre-exponential factor now reads

$$\overline{C}_0(\mathbf{p}_{x0},\mathbf{x}_0,\mathbf{P}_0,\mathbf{Q}_0;\mathbf{\Delta}_x,\mathbf{\Delta}_{p_x}) = 2^{-N_S}\left\{\frac{\det_{N_S}[(1+\overline{\mathbf{c}}_x)(1+\overline{\mathbf{c}}_{p_x})-1]}{\det(\gamma)}\det(\mathbf{D}_{\mathrm{SB}})\right\}^{1/2}, \quad (4.5)$$

and the matrix $\mathbf{D}_{\mathrm{SB}}$ is obtained by taking the limit $\mathbf{c}_{pB},\mathbf{c}_{qB}\to\infty$ in Eq. (B20). In Eq. (4.5), $\overline{\mathbf{c}}_x$ and $\overline{\mathbf{c}}_{p_x}$ denote the γ-scaled Filinov parameters for the system coordinate and momentum, respectively.

If, in addition, the limit $\overline{\mathbf{c}}_x,\overline{\mathbf{c}}_{p_x}\to 0$ is taken in Eqs. (4.4) and (4.5), we obtain an expression which corresponds to a full SC-IVR with respect to the system degrees of freedom and a FB-IVR with respect to the bath degrees of freedom. A conceptually similar mixed SC-FB-IVR for system–bath problems was recently proposed by Thompson and Makri.[88]

Compared to the general GFB-IVR, Eq. (3.4), which involves a $(4N_S+4N_B)$-dimensional phase-space integral, the system–bath GFB-IVR requires only a $(4N_S+2N_B)$-dimensional integration. Moreover, as for the FB-IVR, the fact that the trajectories are continuous in the bath degrees of freedom results in a partial cancellation of the phase of the integrand as well as the magnitude of the prefactor, thus improving the convergence properties of the Monte Carlo integration.

To study the performance of the system–bath GFB-IVR we consider a damped anharmonic oscillator which is obtained by coupling the anharmonic oscillator of Eq. (2.25) to a harmonic bath,

$$H=\frac{p_x^2}{2}+\frac{1}{2}\omega_x^2x^2+ax^3+bx^4 + \sum_j\left[\frac{P_j^2}{2}+\frac{1}{2}\omega_j^2\left(Q_j-\frac{\kappa_j}{\omega_j^2}x\right)^2\right]. \quad (4.6)$$

This model was used by Shao and Makri in their study of the derivative FB-IVR method.[70] It can be viewed as a simple model for vibrational relaxation.

In Eq. (4.6), ω_j denotes the frequency of the jth bath mode. The bath is characterized by its spectral density[89,90]

$$J(\omega)=\frac{\pi}{2}\sum_j\frac{\kappa_j^2}{\omega_j}\delta(\omega-\omega_j) \quad (4.7)$$

which is chosen to be of Ohmic form,

$$J(\omega)=\eta\omega e^{-\omega/\omega_c}, \quad (4.8)$$

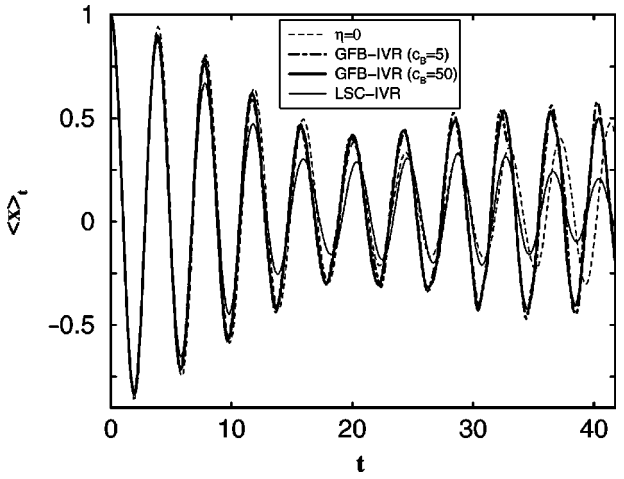

FIG. 7. Dynamics of the average position of an anharmonic oscillator weakly coupled ($\eta=0.1$) to 10 harmonic bath modes. Shown are GFB-IVR results for different values of the Filinov parameter of the bath: $\overline{c}_B=5$ (dashed–dotted line), $\overline{c}_B=50$ (full line), as well as the LSC-IVR/classical Wigner result (thin full line). For comparison the result for the uncoupled ($\eta=0$) anharmonic oscillator is also displayed (thin dashed line).

with coupling strength η and characteristic frequency ω_c. In all numerical results reported below, the characteristic frequency of the bath was chosen as $\omega_c=\omega_x$.

We will focus on the average position of the oscillator, Eq. (4.3), where the initial state is given by a factorized state

$$\rho(0)=|\psi_{iS}\rangle|\psi_{iB}\rangle\langle\psi_{iB}|\langle\psi_{iS}|. \quad (4.9)$$

The initial state for the system is given by Eq. (2.26) and the bath is initially in the ground state

$$|\psi_{iB}\rangle=|0_1\rangle\cdots|0_{N_B}\rangle. \quad (4.10)$$

Let us first study the dependence of the result, as well as the Monte Carlo statistics, on the Filinov parameters of the bath. For this purpose it is not important to model a truly dissipative bath, so we here have discretized the bath spectral density with only 10 oscillators, according to the discretiza-

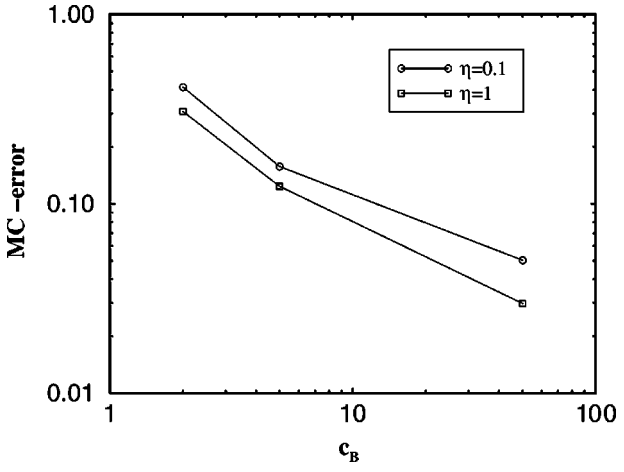

FIG. 8. Estimate of the Monte Carlo fractional error for $\langle x\rangle_t$ at time $t=36.4$ for 30 000 trajectories as a function of the Filinov parameter of the bath $\overline{c}_B$. Shown are results for two different coupling strengths: $\eta=0.1$ (circles), $\eta=1$ (squares).

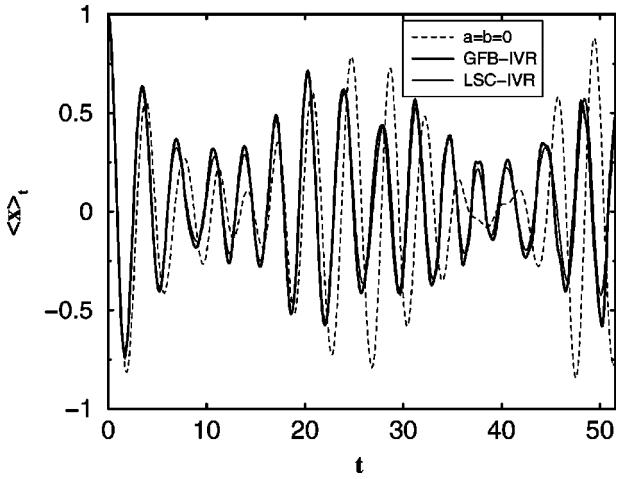

FIG. 9. Dynamics of the average position of an anharmonic oscillator strongly coupled ($\eta=1$) to 10 harmonic bath modes. Shown are LSC-IVR/classical Wigner results (thin full line) as well as results obtained with the system–bath GFB-IVR (thick full line). For comparison the result for the corresponding harmonic system (i.e., $a=b=0$) is also displayed (thin dashed line).

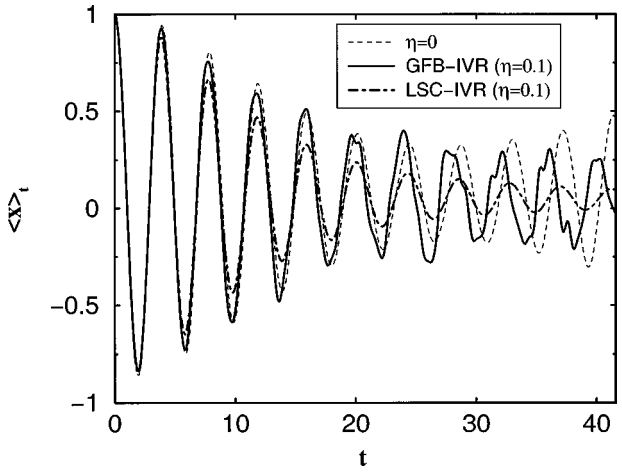

FIG. 10. Dynamics of the average position of an anharmonic oscillator weakly coupled ($\eta=0.1$) to a harmonic bath. Shown are LSC-IVR/classical Wigner results (dashed-dotted line) as well as results obtained with the system–bath GFB-IVR (full line). For comparison the result for the uncoupled ($\eta=0$) anharmonic oscillator is also displayed (thin dashed line).

tion scheme outlined in Ref. 32 (with a maximum bath frequency $\omega_{\max}=2\omega_c$). Figure 7 compares GFB-IVR results in the weak-coupling regime ($\eta=0.1$) obtained with two different values of the Filinov parameter of the bath. For simplicity, the same γ-scaled Filinov parameter was used for all 10 bath modes, i.e., $\bar{\mathbf{c}}_{pB}=\bar{\mathbf{c}}_{qB}=\bar{c}_B\mathbf{1}$. The γ-scaled Filinov parameter for the system was $\bar{c}_x=\bar{c}_{p_x}=1$ in all calculations. Also shown is the LSC-IVR result as well as the quantum mechanical result for the uncoupled system (i.e., $\eta=0$). Due to the weak-coupling, the effect of the bath on the dynamics of the system coordinate is rather small. The comparison with the result for the uncoupled system shows that the damping of the amplitude for $t<20$ is primarily due to the anharmonicity of the system and only amplified to some extent by the interaction with the bath. Another effect of the bath is the phase shift with respect to the uncoupled system and the damping of the recurrence at $t\approx 50$. As for the uncoupled system, the LSC-IVR (and also the FB-IVR which is not shown here) overestimates the damping caused by the anharmonicity and cannot reproduce the recurrence at $t\approx 50$. The small damping due to the interaction with the bath and the phase shift are reproduced rather well, because both effects are also present in the corresponding harmonic system [i.e., $a=b=0$ in Eq. (4.6)] for which the LSC-IVR is exact.

The comparison between the different GFB-IVR calculations demonstrates that there is no significant dependence of the converged result on the Filinov parameter of the bath. The Monte Carlo statistics, and thus the number of trajectories needed to obtain a converged result, on the other hand, depends strongly on the Filinov parameter of the bath. This is illustrated in Fig. 8, which shows the estimate of the Monte Carlo error for $\langle x\rangle_t$ at $t=36.4$ for a fixed number of 30 000 trajectories and three different values of $\bar{c}_B$. The number of trajectories needed to obtain the same Monte Carlo error decreases by almost two orders of magnitude when the Filinov parameter of the bath is increased from $\bar{c}_B=2$ to $\bar{c}_B=50$, thus greatly improving the numerical efficiency.

Whereas in the weak-coupling regime the dynamics is primarily dominated by the anharmonicity of the system and the resulting quantum interference effects, the dynamics behaves more classically if the coupling to the bath is increased. Figure 9 depicts the results for a stronger coupling ($\eta=1$). Thereby, the GFB-IVR results have been obtained using the system–bath variant of this approach (corresponding to the limit $\mathbf{c}_{pB},\mathbf{c}_{qB}\to\infty$) and a system Filinov parameter of $\bar{c}_x=\bar{c}_{p_x}=1$. Also shown is the result for the corresponding harmonic system (i.e., $a=b=0$). In this case the short-time decay of the amplitude of the oscillations is primarily due to the coupling to the bath and the recurrences at $t\approx 30$ and $t\approx 50$ are caused by the finite level density of the discretized bath. The LSC-IVR is seen to be in nearly quantitative agree-

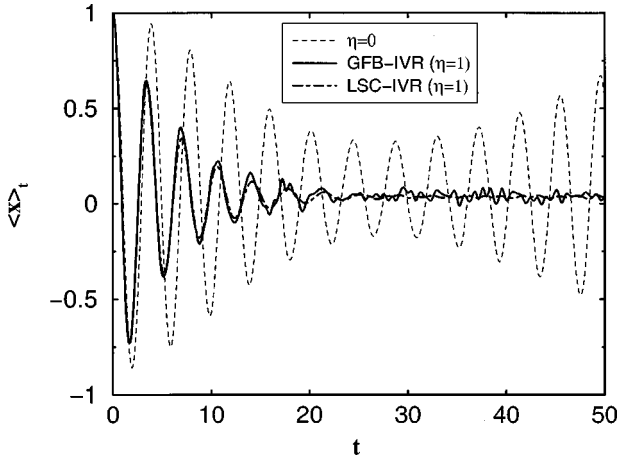

FIG. 11. Dynamics of the average position of an anharmonic oscillator strongly coupled ($\eta=1$) to a harmonic bath. Shown are LSC-IVR/classical Wigner results (dashed–dotted line) as well as results obtained with the system–bath GFB-IVR (full line). For comparison the result for the uncoupled ($\eta=0$) anharmonic oscillator is also displayed (thin dashed line).

ment with the GFB-IVR which demonstrates that for this stronger coupling almost all quantum interference effects have already been quenched by the bath. The absence of quantum interference/coherence in the strong coupling limit also improves the Monte Carlo statistics to some extent as can be seen from Fig. 8.

In the final part of this section we study how the quantum interference/coherence effects present in the dynamics of the uncoupled anharmonic oscillator are quenched by a truly dissipative bath. For this purpose the number of bath modes used in the discretization has to be increased. In several test calculations we have found that within the discretization scheme outlined in Ref. 32 about 100 bath modes and a maximum bath frequency of $\omega_{\max}=5\omega_c$ are sufficient to represent the continuous spectral density for times $t<60$. Because (according to the results shown above) the final result does not depend significantly on the Filinov parameter of the bath we have used the system–bath GFB-IVR (3.4) (corresponding to the limit $\mathbf{c}_{pB},\mathbf{c}_{qB}\rightarrow\infty$) and a system Filinov parameter of $\bar{c}_x=\bar{c}_{p_x}=1$. With this method it was possible to obtain reasonably converged results with 10 000–20 000 trajectories (depending on the coupling strength η), which [in view of the high dimensionality of the Monte Carlo integral $(4N_S+2N_B=204)$] is a rather small number.

Figure 10 shows the dynamics of the average position in the weak-coupling regime ($\eta=0.1$). As was already discussed above, in this regime the dynamics is dominated by the coherent motion of the anharmonic oscillator and the coupling to the bath results in a shift of the frequency, a small damping of the amplitude of the oscillations, and a partial quenching of the recurrence at $t\approx 50$. The semiclassical result shows some spurious structure at longer times which is due to the statistical error.

Figure 11 depicts the same observable for a coupling strength ten times larger ($\eta=1$). In this case all recurrences are quenched by the bath and as the comparison with the LSC-IVR/classical Wigner model shows the result is essentially the classical dynamics of a damped anharmonic oscillator.

V. CONCLUSION

In this work we have studied the capability of two different, recently proposed FB-IVR methods to describe quantum coherence/interference effects. We have found that one can obtain drastically different results depending on whether a derivative or an integral representation of the observable under consideration is used in the derivation of the FB-IVR. To rationalize this finding it was shown that the derivative FB-IVR can be thought of as an approximate version of the LSC-IVR/classical Wigner approach and, therefore, cannot describe quantum interference effects beyond the very short time limit. The FB-IVR based on the integral representation of the observable, on the other, is capable of describing quantum interference effects. Whether even this integral version of the FB-IVR is able to describe *all* interference contained in a semiclassical treatment (i.e., via the full SC-IVR approach), however, depends on the observable under consideration (i.e., on the form of operator $\hat{B}$).

To overcome this limitation of the FB-IVR we have proposed a new, *generalized* FB-IVR approach which can tune continuously between the full SC-IVR and the FB-IVR. It therefore allows one to check whether all interference that can be described semiclassically is included in the calculation. The GFB-IVR combines the capability of the SC-IVR to describe quantum interference effects independent of the particular observable and the better convergence properties of the FB-IVR.

Using a special version of the GFB-IVR which is adapted to system–bath problems, we have studied the quenching of recurrences in the dynamics of an anharmonic oscillator coupled to a harmonic bath. In contrast to the FB-IVR methods, the GFB-IVR was shown to cover both the coherent and incoherent regime, i.e., the recurrences for weak coupling to the bath and the purely classical decay in the strong-coupling regime. Although the motivation for the present model study of this problem was primarily to demonstrate the performance of the method, the occurrence, observability, and quenching of quantum coherence/interference in large molecules or in the condensed phase has been investigated recently in a variety of systems both experimentally and theoretically.[91–99] The results of the present work suggest that the GFB-IVR is well suited to study these phenomena.

ACKNOWLEDGMENTS

This work was supported by the Director, Office of Science, Office of Basic Energy Sciences, Chemical Sciences Division of the U. S. Department of Energy under Contract No. DE-AC03-76SF00098, and by National Science Foundation Grant No. CHE 97-32758. M.T. gratefully acknowledges a Feodor-Lynen fellowship of the Alexander von Humboldt Foundation and thanks W. Domcke for his support. W.H.M. thanks the Emerson Center for Theoretical Chemistry, Emory University, for hosting his very pleasant sabbatical visit during which some of this work was performed.

APPENDIX A: SIMPLIFIED DERIVATIVE FB-IVR

In this section we outline the derivation of the simplified form of the derivative FB-IVR Eq. (2.21). The starting point is the derivative FB-IVR expression Eq. (2.18). The derivative of the integrand in Eq. (2.18) with respect to the momentum jump Δ_p comprises three parts: the derivative of the pre-exponential factor, of the action, and of the coherent state matrix element of the operator $\hat{A}$, i.e.,

$$
\begin{aligned}
&-i\frac{\partial}{\partial\Delta_p}C_0(\mathbf{p}_0,\mathbf{q}_0;\Delta_p)e^{iS_0(\mathbf{p}_0,\mathbf{q}_0;\Delta_p)}\langle\mathbf{p}_0\mathbf{q}_0|\hat{A}|\mathbf{p}_0'\mathbf{q}_0'\rangle\\
&\quad=e^{iS_0(\mathbf{p}_0,\mathbf{q}_0;\Delta_p)}\Big[-i\langle\mathbf{p}_0\mathbf{q}_0|\hat{A}|\mathbf{p}_0'\mathbf{q}_0'\rangle\frac{\partial}{\partial\Delta_p}C_0(\mathbf{p}_0,\mathbf{q}_0;\Delta_p)\\
&\qquad+C_0(\mathbf{p}_0,\mathbf{q}_0;\Delta_p)\langle\mathbf{p}_0\mathbf{q}_0|\hat{A}|\mathbf{p}_0'\mathbf{q}_0'\rangle\frac{\partial}{\partial\Delta_p}S_0(\mathbf{p}_0,\mathbf{q}_0;\Delta_p)\\
&\qquad-iC_0(\mathbf{p}_0,\mathbf{q}_0;\Delta_p)\frac{\partial}{\partial\Delta_p}\langle\mathbf{p}_0\mathbf{q}_0|\hat{A}|\mathbf{p}_0'\mathbf{q}_0'\rangle\Big].
\end{aligned}
\tag{A1}
$$

Note, that all derivatives are taken at the point $\Delta_p=0$. The derivative of the coherent state $|\mathbf{p}_0'\mathbf{q}_0'\rangle$ can be readily obtained

$$\left[\frac{\partial}{\partial\Delta_p}|\mathbf{p}_0'\mathbf{q}_0'\rangle\right]_{\Delta_p=0}=\left[(\hat{\mathbf{q}}-\mathbf{q}_0)\cdot\left(-\gamma\frac{\partial B(\mathbf{q}_t)}{\partial\mathbf{p}_0}+i\frac{\partial B(\mathbf{q}_t)}{\partial\mathbf{q}_0}\right)+i\mathbf{p}_0\cdot\frac{\partial B(\mathbf{q}_t)}{\partial\mathbf{p}_0}\right]|\mathbf{p}_0\mathbf{q}_0\rangle. \tag{A2}$$

Here, we have used the identities,

$$\left[\frac{\partial\mathbf{q}_0'(\mathbf{q}_t,\mathbf{p}_t+\Delta_p[\partial B(\mathbf{q}_t)/\partial\mathbf{q}_t])}{\partial\Delta_p}\right]_{\Delta_p=0}=\frac{\partial\mathbf{q}_0(\mathbf{q}_t,\mathbf{p}_t)}{\partial\mathbf{p}_t}\frac{\partial B(\mathbf{q}_t)}{\partial\mathbf{q}_t}=-\frac{\partial B(\mathbf{q}_t(\mathbf{q}_0,\mathbf{p}_0))}{\partial\mathbf{p}_0}, \tag{A3a}$$

$$\left[\frac{\partial\mathbf{p}_0'(\mathbf{q}_t,\mathbf{p}_t+\Delta_p[\partial B(\mathbf{q}_t)/\partial\mathbf{q}_t])}{\partial\Delta_p}\right]_{\Delta_p=0}=\frac{\partial\mathbf{p}_0(\mathbf{q}_t,\mathbf{p}_t)}{\partial\mathbf{p}_t}\frac{\partial B(\mathbf{q}_t)}{\partial\mathbf{q}_t}=\frac{\partial B(\mathbf{q}_t(\mathbf{q}_0,\mathbf{p}_0))}{\partial\mathbf{q}_0}. \tag{A3b}$$

The derivative of the action is given by

$$\left[\frac{\partial}{\partial\Delta_p}S_0(\mathbf{p}_0,\mathbf{q}_0;\Delta_p)\right]_{\Delta_p=0}=B(\mathbf{q}_t)+\left[\mathbf{p}_0'\cdot\frac{\partial\mathbf{q}_0'}{\partial\Delta_p}\right]_{\Delta_p=0}=B(\mathbf{q}_t)-\mathbf{p}_0\cdot\frac{\partial B(\mathbf{q}_t)}{\partial\mathbf{p}_0}, \tag{A4}$$

where for the last identity we have again used Eq. (A3a). Employing the identity

$$\frac{\partial}{\partial\Delta_p}\det[\mathbf{R}(\Delta_p)]=\det[\mathbf{R}(\Delta_p)]\mathrm{tr}\left[(\mathbf{R}(\Delta_p))^{-1}\frac{\partial}{\partial\Delta_p}\mathbf{R}(\Delta_p)\right], \tag{A5}$$

which is valid for any nonsingular, parameter dependent matrix $\mathbf{R}(\Delta_p)$, the derivative of the pre-exponential factor reads

$$\left[\frac{\partial}{\partial\Delta_p}C_0(\mathbf{p}_0,\mathbf{q}_0;\Delta_p)\right]_{\Delta_p=0}=\frac{1}{2}\ \mathrm{tr}\left(\left[\frac{\partial}{\partial\Delta_p}\mathbf{R}(\Delta_p)\right]_{\Delta_p=0}\right). \tag{A6}$$

Here, the matrix $\mathbf{R}$ is defined by

$$\mathbf{R}(\Delta_p)=\frac{1}{2}\left(\boldsymbol{\gamma}^{1/2}\frac{\partial\mathbf{q}_0'}{\partial\mathbf{q}_0}\boldsymbol{\gamma}^{-1/2}+\boldsymbol{\gamma}^{-1/2}\frac{\partial\mathbf{p}_0'}{\partial\mathbf{p}_0}\boldsymbol{\gamma}^{1/2}-i\boldsymbol{\gamma}^{1/2}\frac{\partial\mathbf{q}_0'}{\partial\mathbf{p}_0}\boldsymbol{\gamma}^{1/2}+i\boldsymbol{\gamma}^{-1/2}\frac{\partial\mathbf{p}_0'}{\partial\mathbf{q}_0}\boldsymbol{\gamma}^{-1/2}\right), \tag{A7}$$

and we have used that $\mathbf{R}(\Delta_p=0)=\mathbf{1}$. Utilizing the identities (A3), the derivative of the pre-exponential factor can be further simplified to

$$\left[\frac{\partial}{\partial\Delta_p}C_0(\mathbf{p}_0,\mathbf{q}_0;\Delta_p)\right]_{\Delta_p=0}=\frac{i}{4}\sum_j\left(\gamma_j\frac{\partial^2B(\mathbf{q}_t)}{\partial p_{0j}^2}+\frac{1}{\gamma_j}\frac{\partial^2B(\mathbf{q}_t)}{\partial q_{0j}^2}\right). \tag{A8}$$

Inserting Eqs. (A4), (A2), and (A8) into Eq. (A1) and integrating by parts, gives

$$C_{AB}^{\mathrm{DFB}}(t)=\int\frac{d\mathbf{q}_0d\mathbf{p}_0}{(2\pi)^N}B(\mathbf{q}_t)\left\{\left[1+\frac{1}{4}\sum_j\left(\gamma_j\frac{\partial^2}{\partial p_{0j}^2}+\frac{1}{\gamma_j}\frac{\partial^2}{\partial q_{0j}^2}\right)\right]\langle\mathbf{p}_0\mathbf{q}_0|\hat{A}|\mathbf{p}_0\mathbf{q}_0\rangle-\sum_j\left(i\gamma_j\frac{\partial}{\partial p_{0j}}+\frac{\partial}{\partial q_{0j}}\right)\langle\mathbf{p}_0\mathbf{q}_0|\hat{A}(\hat{q}_j-q_{0j})|\mathbf{p}_0\mathbf{q}_0\rangle\right\}. \tag{A9}$$

Furthermore, using the identity

$$\left(i\gamma_j\frac{\partial}{\partial p_{0j}}+\frac{\partial}{\partial q_{0j}}\right)\langle\mathbf{p}_0\mathbf{q}_0|\hat{A}(\hat{q}_j-q_{0j})|\mathbf{p}_0\mathbf{q}_0\rangle=-A_H(\mathbf{p}_0,\mathbf{q}_0)+2\gamma_j\langle\mathbf{p}_0\mathbf{q}_0|(\hat{q}_j-q_{0j})\hat{A}(\hat{q}_j-q_{0j})|\mathbf{p}_0\mathbf{q}_0\rangle=\frac{1}{2}\left(\gamma_j\frac{\partial^2}{\partial p_{0j}^2}+\frac{1}{\gamma_j}\frac{\partial^2}{\partial q_{0j}^2}\right)A_H(\mathbf{p}_0,\mathbf{q}_0), \tag{A10}$$

where $A_H(\mathbf{p}_0,\mathbf{q}_0)$ denotes the Husimi distribution of the operator $\hat{A}$ [cf. Eq. (2.22)], we finally obtain

$$C_{AB}^{\mathrm{DFB}}(t)=\int\frac{d\mathbf{q}_0d\mathbf{p}_0}{(2\pi)^N}B(\mathbf{q}_t)\left[\left(1+\frac{N}{2}\right)A_H(\mathbf{p}_0,\mathbf{q}_0)-\sum_j\gamma_j\langle\mathbf{p}_0\mathbf{q}_0|(\hat{q}_j-q_{0j})\hat{A}(\hat{q}_j-q_{0j})|\mathbf{p}_0\mathbf{q}_0\rangle\right]=\int\frac{d\mathbf{q}_0d\mathbf{p}_0}{(2\pi)^N}B(\mathbf{q}_t)\left[1-\frac{1}{4}\sum_j\left(\gamma_j\frac{\partial^2}{\partial q_{0j}^2}+\frac{1}{\gamma_j}\frac{\partial^2}{\partial p_{0j}^2}\right)\right]A_H(\mathbf{q}_0,\mathbf{p}_0). \tag{A11}$$

APPENDIX B: DERIVATION OF THE GFB-IVR

In this Appendix we shall give an outline of the derivation of the GFB-IVR expression, Eq. (3.4). The basic idea of the derivation is to apply the modified Filinov method [cf. Eq. (3.2)] to the full double phase space SC-IVR, Eq. (2.8).

To this end, let us first consider the unitary operator

$$\hat{U}=e^{i\hat{H}t}e^{-i\mathbf{q}_s\hat{\mathbf{p}}}e^{i\mathbf{p}_s\hat{\mathbf{q}}}e^{-i\hat{H}t}. \tag{B1}$$

Inserting the Herman–Kluk SC-IVR, Eq. (2.2), for the two propagators gives the position matrix elements of $\hat{U}$,

$$\begin{aligned}\langle\mathbf{q}_f|\hat{U}|\mathbf{q}_i\rangle=&\int\frac{d\mathbf{q}_0d\mathbf{p}_0}{(2\pi)^N}\int\frac{d\mathbf{q}_t'd\mathbf{p}_t'}{(2\pi)^N}C_t(\mathbf{p}_0,\mathbf{q}_0)C_{-t}(\mathbf{p}_t',\mathbf{q}_t')\\&\times e^{i[S_t(\mathbf{p}_0,\mathbf{q}_0)+S_{-t}(\mathbf{p}_t',\mathbf{q}_t')]}\langle\mathbf{q}_f|\mathbf{p}_0'\mathbf{q}_0'\rangle\\&\times\langle\mathbf{p}_t'\mathbf{q}_t'|e^{-i\mathbf{q}_s\hat{\mathbf{p}}}e^{i\mathbf{p}_s\hat{\mathbf{q}}}|\mathbf{p}_t\mathbf{q}_t\rangle\langle\mathbf{p}_0\mathbf{q}_0|\mathbf{q}_i\rangle\\=&\int d\mathbf{z}\,g(\mathbf{z})e^{if(\mathbf{z})}.\end{aligned} \tag{B2}$$

To cast the integrand into a form where the Filinov transformation can be readily applied, we have defined a $4N$-dimensional vector $\mathbf{z}=(\mathbf{q}_t',\mathbf{p}_t',\mathbf{q}_0,\mathbf{p}_0)$ and the function

$$g(\mathbf{z})=C_t(\mathbf{p}_0,\mathbf{q}_0)C_{-t}(\mathbf{p}_t',\mathbf{q}_t')\prod_{j=1}^{N}\left(\frac{\gamma_j}{\pi}\right)^{1/2}. \tag{B3}$$

The ''phase'' function $f(\mathbf{z})$ involves the action and the exponents of various coherent state matrix elements,

$$\begin{aligned}f(\mathbf{z})=&S_t(\mathbf{p}_0,\mathbf{q}_0)+S_{-t}(\mathbf{p}_t',\mathbf{q}_t')+\mathbf{p}_0'\cdot(\mathbf{q}_f-\mathbf{q}_0')+\mathbf{p}_0\cdot(\mathbf{q}_0-\mathbf{q}_i)+\tfrac{1}{2}(\mathbf{p}_t'+\mathbf{p}_t)\cdot(\mathbf{q}_t'-\mathbf{q}_t)\\&+\frac{i}{2}\sum_j\gamma_j\left[(q_{fj}-q_{0j}')^2+(q_{0j}-q_{ij})^2+\frac{1}{2}(q_{tj}'-q_{tj})^2\right]+\frac{i}{4}\sum_j\frac{1}{\gamma_j}(p_{tj}'-p_{tj})^2+\frac{1}{2}[\mathbf{p}_s\cdot(\mathbf{q}_t'+\mathbf{q}_t)-\mathbf{q}_s\cdot(\mathbf{p}_t'+\mathbf{p}_t)-\mathbf{q}_s\cdot\mathbf{p}_s]\\&+\frac{i}{2}\sum_j\left[\frac{\gamma_j}{2}q_{sj}^2+\frac{1}{2\gamma_j}p_{sj}^2-\gamma_jq_{sj}(q_{tj}'-q_{tj})-\frac{1}{\gamma_j}p_{sj}(p_{tj}'-p_{tj})\right].\end{aligned} \tag{B4}$$

As we have discussed in Sec. III, the modified Filinov method replaces the integral in Eq. (B2) by

$$\langle\mathbf{q}_f|U|\mathbf{q}_i\rangle=\int d\mathbf{z}\,g(\mathbf{z})e^{if(\mathbf{z})}\mathcal{F}(\mathbf{z}), \tag{B5}$$

with the Filinov factor

$$\mathcal{F}(\mathbf{z})=\sqrt{\det\left(1+i\tilde{\mathbf{c}}\frac{\partial^2f}{\partial\mathbf{z}\partial\mathbf{z}}\right)}\exp\left(-\frac{1}{2}\frac{\partial f}{\partial\mathbf{z}}\tilde{\mathbf{c}}\frac{\partial f}{\partial\mathbf{z}}\right), \tag{B6}$$

where the matrix $\tilde{\mathbf{c}}$ contains the Filinov parameters. Defining the vector

$$\mathbf{y}=(\mathbf{q}_0'-\mathbf{q}_f,\mathbf{q}_0-\mathbf{q}_i,\mathbf{q}_t'-\mathbf{q}_t-\mathbf{q}_s,\mathbf{p}_t'-\mathbf{p}_t-\mathbf{p}_s), \tag{B7}$$

we have for the first derivative of f,

$$\frac{\partial f}{\partial\mathbf{z}}=\mathbf{K}\mathbf{y}, \tag{B8}$$

with the $(4N\times4N)$ matrix $\mathbf{K}$ given by

$$\mathbf{K}=\begin{pmatrix}-\frac{\partial\mathbf{p}_0'}{\partial\mathbf{q}_t'}^T+i\frac{\partial\mathbf{q}_0'}{\partial\mathbf{q}_t'}^T\gamma & 0 & \frac{i}{2}\gamma & -\frac{1}{2}\\ -\frac{\partial\mathbf{p}_0'}{\partial\mathbf{p}_t'}^T+i\frac{\partial\mathbf{q}_0'}{\partial\mathbf{p}_t'}^T\gamma & 0 & \frac{1}{2} & \frac{i}{2}\gamma^{-1}\\ 0 & i\gamma & \frac{1}{2}\frac{\partial\mathbf{p}_t}{\partial\mathbf{q}_0}^T-\frac{i}{2}\frac{\partial\mathbf{q}_t}{\partial\mathbf{q}_0}^T\gamma & -\frac{1}{2}\frac{\partial\mathbf{q}_t}{\partial\mathbf{q}_0}^T-\frac{i}{2}\frac{\partial\mathbf{p}_t}{\partial\mathbf{q}_0}^T\gamma^{-1}\\ 0 & 1 & \frac{1}{2}\frac{\partial\mathbf{p}_t}{\partial\mathbf{p}_0}^T-\frac{i}{2}\frac{\partial\mathbf{q}_t}{\partial\mathbf{p}_0}^T\gamma & -\frac{1}{2}\frac{\partial\mathbf{q}_t}{\partial\mathbf{p}_0}^T-\frac{i}{2}\frac{\partial\mathbf{p}_t}{\partial\mathbf{p}_0}^T\gamma^{-1}\end{pmatrix}. \tag{B9}$$

The matrix of second derivatives of f is given by

$$\frac{\partial^2f}{\partial\mathbf{z}\partial\mathbf{z}}=\mathbf{K}\mathbf{J}, \tag{B10}$$

with the matrix $\mathbf{J}$ given by

$$\mathbf{J}=\frac{\partial \mathbf{y}}{\partial \mathbf{z}}=\begin{pmatrix} \frac{\partial \mathbf{q}_0'}{\partial \mathbf{q}_t'} & \frac{\partial \mathbf{q}_0'}{\partial \mathbf{p}_t'} & 0 & 0 \\ 0 & 0 & 1 & 0 \\ 1 & 0 & -\frac{\partial \mathbf{q}_t}{\partial \mathbf{q}_0} & -\frac{\partial \mathbf{q}_t}{\partial \mathbf{p}_0} \\ 0 & 1 & -\frac{\partial \mathbf{p}_t}{\partial \mathbf{q}_0} & -\frac{\partial \mathbf{p}_t}{\partial \mathbf{p}_0} \end{pmatrix}. \tag{B11}$$

As usual in the application of the Filinov method to semiclassical propagators,[45,48,49] we have neglected derivatives of the monodromy matrix in the derivation of Eq. (B10). We note in passing, that the approximate matrix of second derivatives in Eq. (B10) can be shown to be symmetric, as it should be.

The Filinov factor, therefore, reads

$$\mathcal{F}=[\det(1+i\tilde{\mathbf{c}}\mathbf{K}\mathbf{J})]^{1/2}\exp[-\tfrac{1}{2}\mathbf{y}^T\mathbf{K}^T\tilde{\mathbf{c}}\mathbf{K}\mathbf{y}]. \tag{B12}$$

Within the modified Filinov method one can choose a rather arbitrary matrix $\tilde{\mathbf{c}}$ of Filinov parameters, which may also have a weak dependence on the coordinates $\mathbf{z}$. With the choice

$$\tilde{\mathbf{c}}=(\mathbf{K}^T)^{-1}\mathbf{c}\mathbf{K}^{-1}, \tag{B13}$$

where $\mathbf{c}$ denotes the new matrix of Filinov parameters yet to be defined, the Filinov factor simplifies, and one obtains

$$\mathcal{F}=\frac{[\det(\mathbf{K}+i\mathbf{J}^T\mathbf{c})]^{1/2}}{[\det(\mathbf{K})]^{1/2}}\exp[-\tfrac{1}{2}\mathbf{y}^T\mathbf{c}\mathbf{y}]. \tag{B14}$$

To eliminate the dependence of the Filinov factor on the initial and final state parameters $\mathbf{q}_f,\mathbf{q}_i$ we choose the new Filinov matrix $\mathbf{c}$ to be of the form

$$\mathbf{c}=\begin{pmatrix} 0 & 0 & 0 & 0 \\ 0 & 0 & 0 & 0 \\ 0 & 0 & \mathbf{c}_q & 0 \\ 0 & 0 & 0 & \mathbf{c}_p \end{pmatrix}, \tag{B15}$$

with the $N\times N$ diagonal matrices,

$$\mathbf{c}_q=\mathrm{diag}(c_{q1},\ldots,c_{qN}), \tag{B16a}$$

$$\mathbf{c}_p=\mathrm{diag}(c_{p1},\ldots,c_{pN}). \tag{B16b}$$

Using some straightforward but tedious matrix algebra, the product of the $(4N\times 4N)$-dimensional determinant in the Filinov factor $\mathcal{F}$ and the N-dimensional determinants in the pre-exponential factors C_t, C_{-t} can be cast into the following form:

$$\begin{aligned} &C_t(\mathbf{p}_0,\mathbf{q}_0)C_{-t}(\mathbf{p}_t',\mathbf{q}_t')\frac{[\det(\mathbf{K}+i\mathbf{J}^T\mathbf{c})]^{1/2}}{[\det(\mathbf{K})]^{1/2}} \\ &\quad=2^{-N}\left\{\frac{\det[(1+\overline{\mathbf{c}}_q)(1+\overline{\mathbf{c}}_p)-1]}{\det(\gamma)}\det(\mathbf{D})\right\}^{1/2} \\ &\quad=\overline{C}_0(\mathbf{p}_0,\mathbf{q}_0;\boldsymbol{\Delta}_p,\boldsymbol{\Delta}_q), \end{aligned} \tag{B17}$$

which defines the GFB-IVR pre-exponential factor $\overline{C}_0$. Here, $\boldsymbol{\Delta}_p,\boldsymbol{\Delta}_q$denote the momentum and coordinate jumps of the trajectories at time t, i.e.,

$$\mathbf{q}_t'=\mathbf{q}_t+\boldsymbol{\Delta}_q, \tag{B18a}$$

$$\mathbf{p}_t'=\mathbf{p}_t+\boldsymbol{\Delta}_p. \tag{B18b}$$

The diagonal matrices $\overline{\mathbf{c}}_q,\overline{\mathbf{c}}_p$ contain the γ-scaled Filinov parameters,

$$\overline{\mathbf{c}}_q=2\ \mathrm{diag}(c_{q1}/\gamma_1,\ldots,c_{qN}/\gamma_N), \tag{B19a}$$

$$\overline{\mathbf{c}}_p=2\ \mathrm{diag}(c_{p1}\gamma_1,\ldots,c_{pN}\gamma_N), \tag{B19b}$$

and the matrix $\mathbf{D}$ is given by the following combination of monodromy matrix elements:

$$\begin{aligned} \mathbf{D}=&\frac{1}{2}\left(\frac{\partial \mathbf{p}_0'}{\partial \mathbf{p}_t'}-i\gamma\frac{\partial \mathbf{q}_0'}{\partial \mathbf{p}_t'}\right)\frac{(1+\overline{\mathbf{c}}_q)(1+\overline{\mathbf{c}}_p)+1}{(1+\overline{\mathbf{c}}_q)(1+\overline{\mathbf{c}}_p)-1}\left(\frac{\partial \mathbf{p}_t}{\partial \mathbf{p}_0}\gamma+i\frac{\partial \mathbf{p}_t}{\partial \mathbf{q}_0}\right)+\frac{1}{2}\left(\gamma\frac{\partial \mathbf{q}_0'}{\partial \mathbf{q}_t'}+i\frac{\partial \mathbf{p}_0'}{\partial \mathbf{q}_t'}\right)\frac{(1+\overline{\mathbf{c}}_q)(1+\overline{\mathbf{c}}_p)+1}{(1+\overline{\mathbf{c}}_q)(1+\overline{\mathbf{c}}_p)-1}\left(\frac{\partial \mathbf{q}_t}{\partial \mathbf{q}_0}-i\frac{\partial \mathbf{q}_t}{\partial \mathbf{p}_0}\gamma\right) \\ &+\left(\frac{\partial \mathbf{p}_0'}{\partial \mathbf{p}_t'}-i\gamma\frac{\partial \mathbf{q}_0'}{\partial \mathbf{p}_t'}\right)\frac{\gamma(1+\overline{\mathbf{c}}_q)}{(1+\overline{\mathbf{c}}_q)(1+\overline{\mathbf{c}}_p)-1}\left(\frac{\partial \mathbf{q}_t}{\partial \mathbf{q}_0}-i\frac{\partial \mathbf{q}_t}{\partial \mathbf{p}_0}\gamma\right)+\left(\gamma\frac{\partial \mathbf{q}_0'}{\partial \mathbf{q}_t'}+i\frac{\partial \mathbf{p}_0'}{\partial \mathbf{q}_t'}\right)\frac{\gamma^{-1}(1+\overline{\mathbf{c}}_p)}{(1+\overline{\mathbf{c}}_q)(1+\overline{\mathbf{c}}_p)-1}\left(\frac{\partial \mathbf{p}_t}{\partial \mathbf{p}_0}\gamma+i\frac{\partial \mathbf{p}_t}{\partial \mathbf{q}_0}\right). \end{aligned} \tag{B20}$$

Changing integration variables according to Eq. (B18), the GFB-IVR for the unitary operator $\hat{U}$ is given by

$$\begin{aligned} \hat{U}=&\int\frac{d\mathbf{q}_0 d\mathbf{p}_0}{(2\pi)^N}\int\frac{d\boldsymbol{\Delta}_q d\boldsymbol{\Delta}_p}{(2\pi)^N}|\mathbf{p}_0'\mathbf{q}_0'\rangle \\ &\times e^{i[S_t(\mathbf{p}_0,\mathbf{q}_0)+S_{-t}(\mathbf{p}_t',\mathbf{q}_t')]}\overline{C}_0(\mathbf{p}_0,\mathbf{q}_0;\boldsymbol{\Delta}_p,\boldsymbol{\Delta}_q) \\ &\times e^{-(1/2)(\boldsymbol{\Delta}_q-\mathbf{q}_s)\mathbf{c}_q(\boldsymbol{\Delta}_q-\mathbf{q}_s)}e^{-(1/2)(\boldsymbol{\Delta}_p-\mathbf{p}_s)\mathbf{c}_p(\boldsymbol{\Delta}_p-\mathbf{p}_s)} \\ &\times\langle\mathbf{p}_t'\mathbf{q}_t'|e^{-i\mathbf{q}_s\hat{\mathbf{p}}}e^{i\mathbf{p}_s\hat{\mathbf{q}}}|\mathbf{p}_t\mathbf{q}_t\rangle\langle\mathbf{p}_0\mathbf{q}_0|. \end{aligned} \tag{B21}$$

Finally, to obtain the GFB-IVR for a correlation function,

$$C_{AB}(t)=\mathrm{tr}(\hat{A}e^{i\hat{H}t}\hat{B}e^{-i\hat{H}t}) \tag{B22}$$

with a general operator $\hat{B}=B(\hat{\mathbf{p}},\hat{\mathbf{q}})$ we employ the Weyl representation[100] of operator $\hat{B}$,

$$\hat{B}=\int\frac{d\mathbf{q}_s d\mathbf{p}_s}{(2\pi)^N}\tilde{B}(\mathbf{p}_s,\mathbf{q}_s)e^{-i\mathbf{q}_s\hat{\mathbf{p}}}e^{i\mathbf{p}_s\hat{\mathbf{q}}}, \tag{B23}$$

with

$$\tilde{B}(\mathbf{p}_s,\mathbf{q}_s)=\int \mathrm{d}\overline{\mathbf{q}} e^{-i\mathbf{p}_s\cdot\overline{\mathbf{q}}}\langle\overline{\mathbf{q}}+\mathbf{q}_s|\hat{B}\,|\overline{\mathbf{q}}\rangle. \tag{B24}$$

Using the GFB-IVR for $\hat{U}$ and carrying out the integration over $\mathbf{q}_s$ and $\mathbf{p}_s$, we obtain the GFB-IVR for the correlation function,

$$C_{AB}^{\mathrm{GFB}}(t)=\int\frac{\mathrm{d}\mathbf{q}_0\mathrm{d}\mathbf{p}_0}{(2\pi)^N}\int\frac{\mathrm{d}\mathbf{\Delta}_q\mathrm{d}\mathbf{\Delta}_p}{(2\pi)^N}\langle\mathbf{p}_0\mathbf{q}_0|\hat{A}|\mathbf{p}_0'\mathbf{q}_0'\rangle \times e^{i[S_t(\mathbf{p}_0,\mathbf{q}_0)+S_{-t}(\mathbf{p}_t',\mathbf{q}_t')]}\times\overline{C}_0(\mathbf{p}_0,\mathbf{q}_0;\mathbf{\Delta}_p,\mathbf{\Delta}_q) \times\langle\mathbf{p}_t'\mathbf{q}_t'|\hat{\tilde{B}}|\mathbf{p}_t\mathbf{q}_t\rangle, \tag{B25}$$

where the operator $\hat{\tilde{B}}$ is related to $\tilde{B}(\mathbf{p}_s,\mathbf{q}_s)$as follows:

$$\hat{\tilde{B}}=\int\frac{\mathrm{d}\mathbf{p}_s\mathrm{d}\mathbf{q}_s}{(2\pi)^N}\tilde{B}(\mathbf{p}_s,\mathbf{q}_s)e^{i\mathbf{q}_s\hat{\mathbf{p}}}e^{-i\mathbf{p}_s\hat{\mathbf{q}}}e^{-(1/2)(\mathbf{\Delta}_p-\mathbf{p}_s)\mathbf{c}_p(\mathbf{\Delta}_p-\mathbf{p}_s)} \times e^{-(1/2)(\mathbf{\Delta}_q-\mathbf{q}_s)\mathbf{c}_q(\mathbf{\Delta}_q-\mathbf{q}_s)}, \tag{B26}$$

which corresponds to convolution with a Gaussian.

If the operator $\hat{B}$ depends only on coordinates and not on momentum, i.e., $\hat{B}=B(\hat{\mathbf{q}})$, the Weyl transform is given by

$$\tilde{B}(\mathbf{p}_s,\mathbf{q}_s)=\tilde{B}(\mathbf{p}_s)\,\delta(\mathbf{q}_s), \tag{B27}$$

where $\tilde{B}(\mathbf{p}_s)$ is simply the Fourier representation of the function $B(\mathbf{q})$ [cf. Eq. (2.11)]. In this case the GFB-IVR expression can be simplified and we obtain the result (3.4) in Sec. III.

[1] G. Campolieti and P. Brumer, Phys. Rev. A **50**, 997 (1994).
[2] G. Campolieti and P. Brumer, J. Chem. Phys. **107**, 791 (1997).
[3] G. Campolieti and P. Brumer, J. Chem. Phys. **109**, 2999 (1998).
[4] B. R. McQuarrie and P. Brumer, Chem. Phys. Lett. **319**, 27 (2000).
[5] C. J. Margulis, D. A. Horner, S. Bonella, and D. F. Coker, J. Phys. Chem. **103**, 9552 (2000).
[6] K. G. Kay, J. Chem. Phys. **100**, 4377 (1994).
[7] K. G. Kay, J. Chem. Phys. **100**, 4432 (1994).
[8] K. G. Kay, J. Chem. Phys. **101**, 2250 (1994).
[9] K. G. Kay, J. Chem. Phys. **107**, 2313 (1997).
[10] Y. Elran and K. G. Kay, J. Chem. Phys. **110**, 3653 (1999).
[11] Y. Elran and K. G. Kay, J. Chem. Phys. **110**, 8912 (1999).
[12] E. J. Heller, J. Chem. Phys. **94**, 2723 (1991).
[13] S. Tomsovic and E. J. Heller, Phys. Rev. Lett. **67**, 664 (1991).
[14] M. A. Sepulveda, S. Tomsovic, and E. J. Heller, Phys. Rev. Lett. **69**, 402 (1992).
[15] M. A. Sepulveda and E. J. Heller, Phys. Rev. Lett. **101**, 8004 (1994).
[16] M. A. Sepulveda and E. J. Heller, J. Chem. Phys. **101**, 8016 (1994).
[17] W. H. Miller, Adv. Chem. Phys. **25**, 69 (1974).
[18] W. H. Miller, J. Chem. Phys. **95**, 9428 (1991).
[19] B. W. Spath and W. H. Miller, J. Chem. Phys. **104**, 95 (1996).
[20] B. W. Spath and W. H. Miller, Chem. Phys. Lett. **262**, 486 (1996).
[21] X. Sun and W. H. Miller, J. Chem. Phys. **106**, 916 (1997).
[22] X. Sun and W. H. Miller, J. Chem. Phys. **106**, 6346 (1997).
[23] V. S. Batista and W. H. Miller, J. Chem. Phys. **108**, 498 (1998).
[24] X. Sun and W. H. Miller, J. Chem. Phys. **108**, 8870 (1998).
[25] H. Wang, X. Sun, and W. H. Miller, J. Chem. Phys. **108**, 9726 (1998).
[26] X. Sun, H. Wang, and W. H. Miller, J. Chem. Phys. **109**, 4190 (1998).
[27] X. Sun, H. Wang, and W. H. Miller, J. Chem. Phys. **109**, 7064 (1998).
[28] W. H. Miller, Faraday Discuss. Chem. Soc. **110**, 1 (1998).
[29] D. E. Skinner and W. H. Miller, Chem. Phys. Lett. **300**, 20 (1999).
[30] W. H. Miller, J. Phys. Chem. A **103**, 9384 (1999).
[31] V. S. Batista, M. T. Zanni, B. J. Greenblatt, D. M. Neumark, and W. H. Miller, J. Chem. Phys. **110**, 3736 (1999).
[32] H. Wang, X. Song, D. Chandler, and W. H. Miller, J. Chem. Phys. **110**, 4828 (1999).
[33] X. Sun and W. H. Miller, J. Chem. Phys. **110**, 6635 (1999).
[34] V. Guallar, V. S. Batista, and W. H. Miller, J. Chem. Phys. **110**, 9922 (1999).
[35] D. E. Skinner and W. H. Miller, J. Chem. Phys. **111**, 10787 (1999).
[36] H. Wang, M. Thoss, and W. H. Miller, J. Chem. Phys. **112**, 47 (2000).
[37] E. A. Coronado, V. S. Batista, and W. H. Miller, J. Chem. Phys. **112**, 5566 (2000).
[38] M. Thoss, W. H. Miller, and G. Stock, J. Chem. Phys. **112**, 10282 (2000).
[39] R. Gelabert, X. Giménez, M. Thoss, H. Wang, and W. H. Miller, J. Phys. Chem. A **104**, 10321 (2000).
[40] N. T. Maitra, J. Chem. Phys. **112**, 531 (2000).
[41] M. A. Sepulveda and F. Grossmann, Adv. Chem. Phys. **96**, 191 (1996).
[42] F. Grossmann, Comments At. Mol. Phys. **34**, 243 (1999).
[43] S. X. Sun, J. Chem. Phys. **112**, 8241 (2000).
[44] A. R. Walton and D. E. Manolopoulos, Chem. Phys. Lett. **244**, 448 (1995).
[45] A. R. Walton and D. E. Manolopoulos, Mol. Phys. **87**, 961 (1996).
[46] M. L. Brewer, J. S. Hulme, and D. E. Manolopoulos, J. Chem. Phys. **106**, 4832 (1997).
[47] M. L. Brewer, J. Chem. Phys. **111**, 6168 (1999).
[48] M. F. Herman, Chem. Phys. Lett. **275**, 445 (1997).
[49] B. E. Guerin and M. F. Herman, Chem. Phys. Lett. **286**, 361 (1998).
[50] M. F. Herman and E. Kluk, Chem. Phys. **91**, 27 (1984).
[51] E. Kluk, M. F. Herman, and H. L. Davis, J. Chem. Phys. **84**, 326 (1986).
[52] C. F. Spencer and R. F. Loring, J. Chem. Phys. **105**, 6596 (1996).
[53] D. V. Shalashilin and B. Jackson, Chem. Phys. Lett. **291**, 143 (1998).
[54] D. V. Shalashilin and B. Jackson, Chem. Phys. Lett. **318**, 305 (2000).
[55] S. Garashchuck and D. Tannor, Chem. Phys. Lett. **262**, 477 (1996).
[56] S. Garashchuck, F. Grossmann, and D. J. Tannor, J. Chem. Soc., Faraday Trans. **93**, 781 (1997).
[57] S. Garashchuk and D. J. Tannor, Phys. Chem. Chem. Phys. **1**, 1081 (1999).
[58] D. J. Tannor and S. Garashchuck, Annu. Rev. Phys. Chem. **51**, 553 (2000).
[59] J. L. Wirther, J. Chem. Phys. **112**, 7891 (2000).
[60] To estimate the scaling of semiclassical IVR calculations with the number of degrees of freedom N two factors have to be taken into account: Whereas the numerical effort per trajectory scales approximately as N^3 (due to the calculation of the pre-exponential factor), it is still an open question how the Monte Carlo integration over the initial condition of the trajectories scales with the dimensionality of the system. For a recent discussion of this issue, see Refs. 46 and 47.
[61] W. H. Miller, J. Chem. Phys. **53**, 3578 (1970).
[62] D. Thirumalai and B. J. Berne, Annu. Rev. Phys. Chem. **37**, 401 (1986).
[63] C. H. Mak and D. Chandler, Phys. Rev. A **41**, 5709 (1990).
[64] J. D. Doll, D. L. Freeman, and T. L. Beck, Adv. Chem. Phys. **78**, 61 (1994).
[65] C. H. Mak, R. Egger, and H. Weber-Gottschick, Phys. Rev. Lett. **81**, 4533 (1998).
[66] V. S. Filinov, Nucl. Phys. B **271**, 717 (1987).
[67] N. Makri and W. H. Miller, J. Chem. Phys. **87**, 5781 (1987).
[68] N. Makri and K. Thompson, Chem. Phys. Lett. **291**, 101 (1998).
[69] N. Makri and K. Thompson, J. Chem. Phys. **110**, 1343 (1999).
[70] J. Shao and N. Makri, J. Phys. Chem. A **103**, 7753 (1999).
[71] R. Gelabert, X. Giménez, M. Thoss, H. Wang, and W. H. Miller, J. Chem. Phys. **114**, 2572 (2001).
[72] H. Wang, M. Thoss, and W. H. Miller, J. Chem. Phys. **112**, 47 (2000).
[73] H. Wang, M. Thoss, K. Sorge, R. Gelabert, X. Giménez, and W. H. Miller, J. Chem. Phys. **114**, 2562 (2001).
[74] B. J. Berne and G. D. Harp, Adv. Chem. Phys. **17**, 63 (1970).
[75] E. J. Heller, J. Chem. Phys. **65**, 1289 (1976).
[76] R. C. Brown and E. J. Heller, J. Chem. Phys. **75**, 186 (1981).
[77] H. W. Lee and M. O. Scully, J. Chem. Phys. **73**, 2238 (1980).
[78] J. S. Cao and G. A. Voth, J. Chem. Phys. **104**, 273 (1996).
[79] R. E. Cline, Jr. and P. G. Wolynes, J. Chem. Phys. **88**, 4334 (1988).
[80] V. Khidekel, V. Chernyak, and S. Mukamel, in *Femtochemistry: Ultrafast Chemical and Physical Processes in Molecular Systems*, edited by M. Chergui (World Science, Singapore, 1996), p. 507.
[81] Strictly speaking, this derivation has been given so far only within the van Vleck (or coordinate-space) IVR (see Ref. 33). Section III gives (in the limit $\mathbf{c}_q,\mathbf{c}_p\to\infty$) a derivation within the Herman–Kluk IVR.
[82] J. Shao and N. Makri, J. Phys. Chem. A **103**, 9479 (1999).
[83] K. Husimi, Proc. Phys. Math. Soc. Jpn. **22**, 264 (1940).
[84] A. Voros, Phys. Rev. A **40**, 6814 (1989).

[85] Whereas the LSC-IVR/classical Wigner approach is exact for any quadratic Hamiltonian, in the derivative FB-IVR method this depends also on the observable *B*. Equations (2.21) and (2.23) show that the derivative FB-IVR is exact for a quadratic Hamiltonian if the observable *B* depends at most cubic on the coordinate **q**.
[86] This argument is only valid for those degrees of freedom in which the Weyl transform of the operator *B* is localized. If the Weyl transform is delocalized in a coordinate (or a momentum) [such as, for example, for the calculation of the density, where $\tilde{B}(\Delta_p)=e^{i\Delta_p q}$], all coordinate (momentum) jumps will contribute.
[87] In contrast to the full double phase space SC-IVR, the FB-IVR (and therefore also the GFB-IVR for large Filinov parameters) is not manifestly positive. As for the LSC-IVR the occurrence of negative parts in the density $\rho_t(x)$ is an indication that the approximation involved (in this case the additional stationary phase approximation of the FB-IVR) is no longer valid.
[88] K. Thompson and N. Makri, Phys. Rev. E **59**, R4729 (1999).
[89] A. J. Leggett, S. Chakravarty, A. T. Dorsey, M. P. A. Fisher, A. Garg, and W. Zwerger, Rev. Mod. Phys. **59**, 1 (1987).
[90] U. Weiss, *Quantum Dissipative Systems* (World Scientific, Singapore, 1993).
[91] M. H. Vos, F. Rappaport, J.-C. Lambry, J. Breton, and J.-L. Martin, Nature (London) **363**, 320 (1993).
[92] D. M. Jonas, S. E. Bradford, S. A. Passino, and G. R. Fleming, J. Phys. Chem. **99**, 2954 (1995).
[93] D. C. Arnett, P. Vohringer, and N. F. Scherer, J. Am. Chem. Soc. **117**, 12262 (1995).
[94] A. Lucke, C. H. M. R. Egger, J. Ankerhold, J. Stockburger, and H. Grabert, J. Chem. Phys. **107**, 8397 (1997).
[95] S. Spörlein, W. Zinth, and J. Wachtveitl, J. Phys. Chem. B **102**, 7492 (1998).
[96] B. Wolfseder, L. Seidner, G. Stock, W. Domcke, M. Seel, S. Engleitner, and W. Zinth, Chem. Phys. **233**, 323 (1998).
[97] Y. Jung, R. J. Silbey, and J. Cao, J. Phys. Chem. A **103**, 9460 (1999).
[98] I. V. Rubtsov and K. Yoshihara, J. Phys. Chem. A **103**, 10202 (1999).
[99] M. Arndt, O. Nairz, J. Vos-Andreae, C. Keller, G. van der Zouw, and A. Zeilinger, Nature (London) **401**, 680 (1999).
[100] H. Weyl, Z. Phys. **46**, 1 (1927).